Title:

Eight Unexpected Selenoprotein Families in ABC transport, in Organometallic Biochemistry in *Clostridium difficile* and other anaerobes, and in Methylmercury Biosynthesis.

Authors:

Daniel H. Haft (corresponding author)
National Center for Biotechnology Information
National Library of Medicine
NIH
Bethesda, MD 20892
daniel.haft@nih.gov

Marc Gwadz
National Center for Biotechnology Information
National Library of Medicine
NIH
Bethesda, MD 20892

Abstract:

A novel protein family related to mercury resistance protein MerB, which cleaves Hg-C bonds of organomercurial compounds, is a newly recognized selenoprotein, typically seen truncated in sequence databases at CU (cysteine-selenocysteine) dipeptide sites fifty residues before the true C-terminus. Inspection shows this protein occurs in a nine-gene neighborhood conserved in more than fifty bacterial species, taxonomically diverse but exclusively anaerobic, including spirochetes, deltaproteobacteria, and Gram-positive spore-formers *Clostridium difficile* and *C. botulinum.* Three included families are novel selenoproteins in most instances, including two ABC transporter subunits, one a substrate-binding protein with another CU motif, the other a permease subunit with selenocysteine at the substrate-gating position. Phylogenetic profiling shows a strong pattern of co-occurrence with Stickland metabolism selenoproteins, but an even closer link to a group of 8Fe-9S cofactor-type double-cubane proteins. These 8Fe-9S enzymes vary in count and in genome location but frequently sit next to the nine-gene locus. We have named the locus SAO, because of the Selenocysteine-Assisted Organometallic (SAO) biochemistry implied by an uptake ABC transporter with apparent metal-binding selenocysteines, complementary metal efflux pump SaoE, the MerB-like cytosolic enzyme now called SaoL, and comparative genomics signatures suggesting energy metabolism rather than metal resistance. Hypothesizing cycles of formation and dismutation of organometallic compounds involved in fermentative metabolism, we examined methylmercury formation proteins, and discovered most HgcA proteins are selenoproteins as well, with a CU motif N-terminal to the previously predicted start. Seeking additional rare and overlooked selenoproteins, tricky because of their rarity, could help reveal more candidate cryptic biochemical processes.

Introduction:

Clostridioides (*Clostridium*) *difficile*, an important intestinal pathogen, can become prevalent after patients are exposed to certain antibiotics, and then maintain itself in a diarrheal disease-causing dysbiosis for extended periods. Several important principles of *C. difficile*'s survival as an obligate anaerobe in the intestinal milieu are well described (1-3). Much of its energy generation depends on the extraction of energy substrates refractory to anaerobic oxidation by most other bacteria. *C. difficile* is a specialist in finding respiratory sinks, and several pathways it contains have been examined in detail. For one, it performs acetogenesis, converting carbon dioxide (CO_2), via carbon monoxide (CO), plus hydrogen (H2), to acetyl-CoA through the Wood-Ljundahl pathway (WLP) (1). From acetyl-CoA, *C. difficile* does not simply export acetic acid, but instead performs further transformations, generating both ethanol and butyrate (2). *C. difficile* also performs Stickland-type fermentations of a wide variety of amino acids (1,4), coupling some transformations to H+/Na+ transport, which creates gradients that it uses to generate ATP.

Several key proteins used in Stickland reactions invariably require selenium, with key selenoproteins including glycine reductase subunits GrdA and GrdB, sarcosine reductase subunit GrdF, and proline reductase subunit PrdB. Selenium in the form of selenocysteine is used in *C. difficile* also in a formate dehydrogenase and the selenophosphate synthase enzyme SelD, two of the most widespread selenoproteins in bacteria (5). In addition to selenocyteine-containing enzymes, *C. difficile* has the YqeB and YqeC gene pair for preparing the labile selenium-containing molybdenum cofactor (Se-cofactor) for

enzymes referred to collectively as selenium-dependent molybdenum hydroxylases (SDMH) (6,7). Characterized SDMH enzymes of this type include nicotinic acid hydroxylase from *Clostridium barkeri* (8), purine hydroxylase from *Clostridium purinolyticum* (9), and xanthine dehydrogenase EF2570 from *Enterococcus faecalis (10)*. The protein CAJ70074.1 from *C. difficile* is 59 % identical to the *E. faecalis* enzyme and annotated as functionally equivalent. However, that enzyme is just one of several candidate SDMH in the proteome, suggesting that several additional selenium-dependent pathways remain to be catalogued in clostridial species.

In light of the broad interest in the metabolic capabilities of *C. difficile*, in the relationships between microbiome-mediated fermentations in the gut and metabolites appearing in host serum, and in new protein family discoveries that expand the selenoproteome (5,11), we were surprised to encounter an apparently overlooked system of nine proteins, six from families whose memberships include selenoproteins some to most of the time, and to find the system closely associated with a still only partly characterized metalloenzyme family that features the highly unusual 8Fe-9S cofactor. The system's overabundance of Cys-rich and Sec-containing motifs, its MerB-related putative organometallic lyase, its putative metal import and export transporters, and its correlations with anaerobic metabolism, Stickland fermentation, and 8Fe-9S cluster proteins suggest something novel. It suggests a system that exists for metabolic throughput and energy generation rather than heavy metal resistance, one that transports metal-containing compounds or ions both inwards and outwards, a still-undescribed Selenocysteine-Assisted Organometallic (SAO) system whose pathways may involve transient formation and later dismutation of organometallic compounds.

Methods

Discovery of novel selenoproteins

Groups of proteins with sequence similarity were detected by BLAST (12) or HMMER (13) searches and aligned using Clustal-W (14) or muscle (15). Multiple sequence alignments were examined, made non-redundant, and trimmed in belvu (16). Any sequence with an unexpected N-terminal or C-terminal truncation, such that the missing region covers what would otherwise be a strongly conserved cysteine (Cys or C) or selenocysteine (Sec or U) residue was considered a candidate selenoprotein. Review of such families looked for 1) at least ten candidate selenoprotein examples in each family, 2) universal presence of TGA (100%) in the DNA encoding the putative selenocysteine site, 3) strong protein-protein sequence similarity running through the putative U residue, showing conservative substitution of amino acid residues and consistent average protein lengths for selenoprotein vs. non-selenoprotein members of the same family. In the cases of a fifth (SaoC) and six (SaoX) selenoprotein in an operon, requirements were relaxed somewhat, but still reported. For SaoC, continued alignment past the Sec residue is not required because the identified Sec residue is the C-terminal residue.

SECIS element verification

Messenger RNA sequence starting from the UGA codon position were examined manually for regions capable of forming RNA structures that could serve as selenocysteine insertion (SECIS) elements, using dotter (17) for visualization. Searches for SECIS elements were attempted at http://gladyshevlab.org/SelenoproteinPredictionServer/ (18) with a variety of settings but were unsuccessful for both the novel selenoproteins described here and for previously several previously described selenoproteins. Server-based confirmation of putative novel selenoproteins was therefore not used as a criterion for selenoprotein identification.

115
116 *Reference data for comparative genomics studies*
117 Three collections of representative genomes were used. The larger collection is the full set of
118 PGAP-annotated prokaryotic assemblies that are in the RefSeq collection (references) and identified as
119 representative, that is, passing a variety of quality assurance metrics on the quality of structural and
120 functional annotation and then chosen as the single representative of that species. This collection
121 contained 15,511 genomes as of May 5, 2022. We will refer to the snapshot from that date, a static set,
122 as "the calibration set". It is used by NCBI biocurators during the construction, curation, review, and
123 testing of protein family models being developed for PGAP (19).
124
125 A collection very similar to the calibration set is available for BLAST searching as "RefSeq Select
126 proteins (refseq_select)" at NCBI's Web BLAST page
127 https://blast.ncbi.nlm.nih.gov/Blast.cgi?PROGRAM=blastp. Only bacterial assemblies within that
128 collection are relevant to this study. We will refer to this larger set of assemblies as "RefSeq Select."
129
130 Lastly, a collection of 3217 assemblies was built in July 2018 for studies using the algorithm
131 Partial Phylogenetic Profiling (PPP), a data-mining algorithm that looks for statistical evidence that one
132 protein family regularly co-occurs with another, while performing on-the-fly optimizations of protein
133 family size that best reveal what patterns of co-occurrence may be inherent in the genomic data (20,21).
134 We refer to this collection of prokaryotic proteomes as "the PPP reference set."
135
136 *Protein Family Definition*
137 Each protein family definition was created by first building a multiple sequence alignment of
138 representative sequences, then trimming off poorly conserved end regions and eliminating highly
139 redundant sequences. Protein profile hidden Markov models (HMMs) were constructed from these
140 curated alignments, using HMMER3 (13). Curator examination of well-conserved genomic regions was
141 used to guide construction of HMMs that provide sharp separation between members of each family
142 and additional homologs outside the family, if any exist, and then to set cutoffs that would limit or
143 eliminate both false-positive and false-negative scoring of potential member proteins of each
144 family. For families in which previously missed identifications of selenocysteine-containing full-length
145 versions of protein sequences complicated calibration, we first determined what the corrected
146 sequences should be, and then used the corrected sequences to set cutoffs.
147
148 *Partial Phylogenetic Profiling (PPP)*
149 PPP was performed in order to see what proteins show the most consistent patterns of co-
150 occurrence with the MerB-like selenoprotein family (SaoL) and with the rest of our newly built protein
151 families from its conserved gene neighborhood. PPP was performed by using a query profile of 33
152 species encoding the CysCys-COOH protein (SaoC), among the 3217 of the PPP reference set.
153
154 BLAST search results needed for PPP were generated for all proteins from each of five
155 taxonomically diverse RefSeq-annotated assemblies: GCF_000009205.1 (*Clostridioides difficile* 630),
156 GCF_000325665.1 (*Brachyspira pilosicoli* P43/6/78), GCF_001754075.1 (*Merdimonas faecis*),
157 GCF_001940565.1 (*Tissierella creatinophila* DSM 6911), and GCF_000014965 (*Syntrophobacter*
158 *fumaroxidans* MPOB). The PPP software uses the algorithm previously described (20,21) but is a custom
159 implementation that works within NCBI infrastructure, with dependencies that include use of in-house
160 compute farms and relational databases.
161

The PPP algorithm examines how consistently two protein families co-occur, being both present or both absent, across large numbers of other genomes. The first family is represented by its phylogenetic profile, that is, by the list of all genomes found to contain the family. This profile provides the reference standard used when PPP searches the proteome for any protein that can be seen as belonging to a second family occurring in a similar set of genomes, so the profile functions as a query. PPP examines every protein in a proteome, one at a time, and finds the best possible score for that protein. To find that optimized score, it scans down the descending list of best BLAST hits, finds the genome of origin for every homolog, and computes odds according to the binomial distribution that such an overrepresentation of YES genomes could have been seen purely by chance. For each protein in the genome, the reported score comes from the depth in the scan down the BLAST hits list where the negative of the log of the computed odds hits the highest possible score.

PPP scores are computed for all proteins annotated in a genome, sorted in order from the highest (most significant) PPP score to lowest. Because proteomes from related species, or inhabiting related environments that require similar adaptations, may have considerable overlap in protein family content, no assumption of statistical independence can be made for the distribution of two different protein families among the different proteomes in the test set. Consequently, PPP scores as they are computed, uncorrected, have a high background, and must be used only by comparison to scores for other proteins from the same proteome. The top tier of proteins, those scoring well above background, are reviewed under the assumption that joint appearances across large numbers of genomes may point to a mechanistic connection between those proteins and the one used as the basis for the query profile. Results are interpreted by investigating proteins that score far above this background, after which we build new HMM-based protein family definitions as necessary, with cutoffs set manually only after review of gene neighborhoods and molecular phylogenetic trees.

The assemblies used for PPP have structural annotation that predates the discovery reported here of six new selenoprotein-containing protein families, and are used without any special correction. PPP therefore performs computation on part-length versions of selenoproteins, missing regions either N-terminal or C-terminal to the selenocysteine-encoding UGA codon.

A standard warning applies for all use of PPP, namely, problems that make BLAST search results less reliable make PPP results less reliable. Concerns include suboptimal structural annotation (failure to find all coding regions with correct start sites), repetitive sequences or low-complexity sequence in proteins, or that the order of best hits as computed by BLAST somehow fails to perform as well as desired to separate members of one branch of a large protein family from other branches. For this reason, the BLAST distance-based definitions of protein families that PPP weighs on the fly during computation should be replaced by curator-constructed and validated protein family definitions for downstream uses such as genome annotation and comparative genomics.

Structure Prediction

3D Protein structure predictions were obtained via Alpha Fold v2 installed on the NIH Biowulf supercomputing cluster, using all available sequence and template databases. The highest confidence 3D model of each protein prediction was submitted to VAST Search (https://www.ncbi.nlm.nih.gov/Structure/VAST/vastsearch.html) (22), which compares the 3D coordinates of a submitted protein structure (including those modeled by AlphaFold) to all solved 3D structures in NCBI's Molecular Modeling Database, to help identify structure neighbors of interest. 3D

visualization was performed using iCn3D for most proteins (23,24), while the structural alignment and overlay visualization of SaoP with the MetI dimer used ChimeraX (25).

Results:

MerB-like selenoprotein (SaoL)

Pfam (26) model PF03243 identifies proteins of the MerB family. Characterized members of that family described in the literature (27) are organomercurial lyases (EC 4.99.1.2) able to cleave substrates such as methyl-mercury. MerB-like proteins WP_004454659.1 from *Clostridioides difficile* (Firmicutes), WP_041443257.1 from *Syntrophobacter fumaroxidans* (Deltaproteobacteria), and WP_228369505.1 from *Brachyspira pilosicoli* (Spirochaetes) predicted previously by PGAP (19) represented a distinct branch within the alignment of MerB-like proteins. All predicted proteins in this branch were somewhat shorter than the typical MerB, averaging 197 residues in length, and all ended in a perfectly aligned Cys. Since some selenoproteins contain a CU (Cys-Sec) or UC (Sec-Cys) dipeptide motif, we investigated the possibility that all were, in fact, previously unrecognized and therefore improperly truncated selenoproteins. In every case, the original stop codon was UGA, which can encode selenocysteine, followed by a resumption of the open reading frame. Translations with a single UGA codon interpreted as selenocysteine produced alignments with homology extending to the C-terminus of MerB-like proteins such as WP_008520765.1 of *Jonquetella anthropic*, WP_208119251.1 of *Spirabiliibacterium pneumoniae*, and WP_151052138.1 of *Neisseria zalophi*.

By examining the genomic regions surrounding WP_004454659.1, WP_041443257.1, WP_228369505.1, and their closest homologs, we discovered that the sequences can be treated as the founding members of a novel protein family that serves as a molecular marker for a large conserved gene neighborhood. The neighborhood occurs 52 times in a collection 15,511 representative prokaryotic genome assemblies. This is just 0.3 % of species, all anaerobic, skewed heavily toward the Firmicutes but broadly distributed. Examination of neighborhoods showed that the sequence mentioned above from *Jonquetella anthropici*, WP_008520765.1, shares the same gene neighborhood and is the lone member of the SaoL family that that has a CC rather than CU motif. *Jonquetella anthropici* does have a selenocysteine incorporation system for production of other selenoproteins.

Surprisingly, a member of this MerB-like (seleno)protein is found in only 45 of the 52 conserved regions. It occurs as a selenoprotein in 44 of the 45 (98%). The full list of hits in RefSeq can be found by searching Protein Family Models at https://www.ncbi.nlm.nih.gov/protfam for hidden Markov model NF040728. The nine novel protein families of the neighborhood, with suggested gene symbols, protein names, accession numbers of HMMs identifying protein family members, and other notes, are listed in **Table 1**. All members of all nine family are found exclusively in bacteria. Note that we have added corrected full-length sequences that span the selenocysteine insertion site as reference information for PGAP, so the pipeline now correctly produces full-length proteins when PGAP annotates new prokaryotic genome assemblies entering RefSeq or when it does its regular reannotations of existing assemblies.

The MerB-like selenoprotein turned out to be the first novel selenoprotein we found in its conserved gene neighborhood. It serves as a molecular marker for the presence of an extended locus at least nine genes in length, several others of which also encode selenoproteins, as will be described. We

254 infer that the system on the whole acts on organometallic (probably organomercurial) compounds, as
255 MerB itself does, and suggest the term ***SAO*** (**S**elenocysteine-**A**ssisted **O**rganometallic) as a shorthand
256 name for the system on the whole. For this MerB-like protein, we suggest the name "SaoL", for
257 "**S**elenocysteine-**A**ssisted **O**rganometallic Lyase."
258
259 *3D structural prediction for SaoL.*
260 The corrected, full-length, selenocysteine-containing protein SaoL of *Clostridioides difficile* 630 is
261 WP_238476746.1, 213 amino acids long with a CU motif at position 161-162. The U in WP_238476746.1
262 was changed to C, producing a sequence we designate $SaoL_{Cdiff}$Sec162Cys, in order to avoid having
263 AlphaFold treat the selenocysteine as X. **Figure 1** shows structures for $SaoL_{Cdiff}$Sec162Cys, as predicted
264 by AlphaFold2, and for MerB from *Escherichia coli* plasmid R831b, solved crystallographically with a
265 bound mercury atom as PDB structure 3F0P. The two sequences, although homologous and both
266 recognized by Pfam model PF03243, share less than 15% pairwise identity in amino acid sequence.
267 However, homology is readily detected by BLAST search with $SaoL_{Cdiff}$ or HMM NF040728 vs. sequences
268 represented in PDB, while VAST (Vector Alignment Search Tool) (28) finds the similarity of the two 3D
269 structures.
270
271 MerB enzymes acts as organomercurial lyases for methylmercury and a broad variety of
272 related organomercurial substrates. MerB's binding to and positioning of active site residues at the
273 mercury atom is paramount. It is notable that MerB will bind other heavy metal atoms where it binds
274 Hg (29), a single amino acid change at the metal-binding site can convert MerB to a copper-binding
275 enzyme (29), and the ability of heavy metal atoms for bond covalently to carbon is not limited to
276 mercury, but includes also, for example, arsenic and cobalt. The replacement of Cys by Sec at a site
277 contacting the heavy metal atom may be a profound change, so it increases suspicion that the
278 physiologically relevant substrate profile may not be restricted to organomercurial compounds. Indeed,
279 mercury resistance operons frequently are encoded on plasmids, and for well-studied human pathogens
280 tend be present only sporadically. By contrast, the SAO system in *C. difficile* strains is chromosomal,
281 surrounded by housekeeping-like rather than mobilome-like genes, and preserved in 3279 of 3343
282 genome assemblies (98%) for that species annotated by PGAP for the RefSeq collection.
283
284
285 *CD2361 family ABC transporter ATP-binding protein (SaoA)*
286 Homologs of CD2361 (WP_003430772.1) are the ATP-binding subunit of an adjacent ABC
287 transporter of unknown substrate. None of the members of this family are selenoproteins, and that is
288 expected. The ATP subunit energizes high-affinity transport by its effects on other subunits, and it does
289 not interact directly with substrate. High sequence similarity to other nitrate/sulfonate/taurine group
290 ABC transporter subunits helps determine that adjacent genes likely also encode subunits of an ABC
291 transporter, although the substrate remains unknown. We suggest the name SaoA (**SAO** system **A**TP-
292 binding protein).
293
294 *ABC transporter permease selenoprotein (SaoP)*
295 The adjacent ABC transporter permease subunit, originally predicted to be 209 amino acids in C.
296 difficile (WP_003430774.1), was corrected to a length of 268 by translation through the selenocysteine-
297 encoding UGA codon. Members of the family are mutually more than 45% identical to each other. In a
298 few members of the family (WP_008522719.1, WP_015556508.1), Cys is present rather than Sec, but
299 the majority of family members are selenoproteins. We suggest the name SaoP (Selenocysteine-Assisted
300 Organometallic transport Permease).
301

302 Pairwise sequence alignment of the sequence to proteins with a solved crystal structure, such as
303 the MetI subunit of the MetNI methionine ABC transporter shows the highly conserved selenocysteine
304 in WP_003430774.1 aligning within a residue of Met-163 of MetI. MetI forms a homodimer. In the
305 solved conformation, open toward the cytosol and closed on the extracellular face, side chains of the
306 Met-163 residues to the two MetI monomers pack together, as that residue performs a gating function
307 (30).
308
309 The positioning of SaoP's selenocysteine side chain in a gating position becomes even more vivid
310 after structure prediction. Because SaoP is the only ATP transporter permease in the SAO locus, it too is
311 expected to form a homodimer. The top-scoring AlphaFold prediction for the SaoP homodimer, as seen
312 in **Figure 2**, puts the permease in an open-inward (toward the cytosol) configuration. The panel on the
313 left shows excellent superposition with the solved structure 3DHW of MetI. The alignment of SaoP to
314 MetI based on their structures aligns Met-163 of MetI in PDB crystallographic structure 3DHW to Cys-
315 210 (standing in for Sec-210 for software compatibility) in the AlphaFold structure of SaoP. The right
316 panel shows a top-down view of the SaoP dimer. The selenocysteine side chains of the two SaoP
317 monomers appear close enough to form a diselenide bond, or to have both contact the same putative
318 metal atom of a possible organometallic transporter substrate.
319
320 Selenocysteine residues are extremely uncommon in any type of transporter. We know of no
321 previous example of an ABC transporter subunit containing a selenocysteine residue. The presence of
322 two selenocysteine residues, positioned so they can form a diselenide bond, or both can serve as ligands
323 to the same moiety in whatever substrate is being imported, is striking. This positioning of
324 selenocysteine at such a critical site suggest that chemistry involving the pair of selenium atoms is
325 critical to both gating and transport by this novel permease.
326
327
328 *ABC transporter substrate-binding protein (SaoB)*
329 Upstream of the permease subunit is a protein we judge to be the substrate-binding protein
330 (SBP) of the ABC transporter whose other subunits are SaoA and SaoT. The two previously predicted
331 proteins in *C. difficile*, WP_009897548.1 and WP_009897547.1, are actually N-terminal and C-terminal
332 regions within WP_239591066.1, which we were able to make full length after recognizing the
333 selenocysteine-containing nature of the protein. We designate this protein SaoB (Selenocysteine-
334 Assisted Organometallic transport substrate-Binding protein). Homology between SaoB and previously
335 reported ABC transporter SBPs is remote. Two rounds of PSI-BLAST (12) of WP_239591066.1 vs.
336 RefSeq_Select, using an inclusion threshold of 1e-8, followed by multiple sequence alignment of
337 homologs with E-values 0.1 or better, yielded 85 sequences, which became 49 after removing
338 fragmentary sequences and redundant protein sequences more than 80% identical to others. The
339 resulting multiple alignment showed distant but convincing sequence similarity across the full length of
340 the multiple sequence alignment (data not shown), suggesting homologous origin and similar 3D
341 structure, to proteins such as WP_048312536.1, which in turn has very strong sequence similarity (E-
342 value < 1e-43) to SBP with solved structures, such as PDB:3VVE and PDB:4ZV2.
343
344 The selenocysteine-containing motif in SaoB family protein WP_009897548 is CU, echoing the
345 CU motif seen in the MerB family selenoproteins. As with the permease subunit, in which two Sec or Cys
346 residues come together by dimerization, the substrate-binding protein also seems able to provide two
347 (seleno)cys ligands to a single metal atom. More than 60 % of the members of the SaoB family are

348 selenoproteins. As with ABC transporter permease subunits, we know of no previous example of any
349 ABC transporter SBP containing selenocysteine.
350
351 We performed structural predictions for $SaoB_{Cdiff}$Sec72Cys, a sequence derived from the *C.*
352 *difficile* selenoprotein WP_239591066.1. A long N-terminal region including the signal sequence was
353 predicted at low confidence and apart from the main globular structure, so the signal sequence was
354 removed and fold prediction repeated. **Figure 2** shows to the left a structural prediction for
355 $SaoB_{Cdiff}$Sec72Cys with the signal sequence removed, and the right, a prediction for SaoX protein
356 WP_004454662.1 with its lipoprotein signal sequence removed. A VAST search for PDB structures
357 similar to the prediction made for $SaoB_{Cdiff}$Sec72Cys shows that the most closely related structures
358 belong to other ABC transporter substate-binding proteins, confirming observations made by sequence
359 comparisons. In $SaoB_{Cdiff}$Sec72Cys, cysteine residues occur at positions 71, 72, 91, and 174. The first
360 three Cys residues are well-conserved in a multiple sequence alignment of SaoB family proteins, and
361 their side chain sulfur atoms are shown to be close to each other in the fold prediction, packing around a
362 probable substrate-binding site. Cys-174 is not conserved in multiple alignments, and is therefore not
363 highlighted in Figure 2, but comparison to other solved crystal structures suggests it also is a likely close
364 contact to substrate. The companion image in Figure 2, from SaoX (described below), which also has
365 conspicuous conserved Cys residues, shows a similar convergence of Cys residue side chains in the
366 substrate-binding pocket.
367
368 *CD2365 family substrate-binding (lipo)protein (SaoX)*
369 Members of the family of CD2365 from *C. difficile* 630 (CAJ69250.1) nearly always are
370 lipoproteins. The family is related to a number of ABC transporter substrate-binding proteins, which
371 would make it an extra SBP in a system with only one ABC transporter permease subunit and only one
372 ATP-binding protein. The protein is designated SaoX (SAO system eXtra binding-protein). Because SaoX
373 is a lipoprotein, it was studied as part of the *C. difficile* lipoproteome. It was found to be expressed in
374 vegetative cells and at even higher levels in spores (31,32). This lipoprotein may serve, fortuitously, as a
375 marker for expression of the SAO system. It seems to suggest that the whole operon is transcriptionally
376 active and expressed as protein, and that the system has a meaningful role in host cell metabolism, even
377 during spore outgrowth. SaoX has a conserved CC motif at positions 224-225. Cys-192 has an adjacent
378 Cys at 191 in about half of SaoX sequences. SaoB and SaoX therefore differ from any of 27 other
379 annotated ABC transporter SBP in the *Clostridioides difficile* 630 genome in having a
380 CC or CU motifs. Double-cysteine motifs appear to be uncommon in SBP, and do not occur in the 38 ABC
381 transporter SBP of *Escherichia coli* K-12.
382
383 Of the 52 annotated bacterial assemblies in the calibration data set that contain the nine-gene
384 system, a single species, *Negativibacillus massiliensis*, appeared to lack a substrate-binding lipoprotein
385 from this family as annotated. What it had instead as originally annotated is two consecutive tandem
386 pairs of proteins, WP_022132697 and WP_022132698, followed by WP_022132699 and
387 WP_022132700, with the upstream protein terminating in a TGA codon that aligns to the second Cys of
388 the more N-terminal CC motif in the CD2365. Correcting the structural annotation in *N. massiliensis*
389 gives two novel putative selenoproteins, WP_248000900 and WP_248000901, full-length homologs of
390 CD2365, with TU at 191-192 where many homologs have CC.
391
392 *CD2367 family efflux transporter* (SaoE)
393 CD2367, encoded two genes further upstream, appears to be a transmembrane transporter, but
394 not an ABC transporter. According to TCDB (33), members of that family, such as WP_022618526.1 from

395 *C. difficile*, belong to the Organo-Arsenical Exporter (ArsP) family. While members of CD2367's family do
396 not include selenoproteins, the most closely related described family among characterized proteins, the
397 SO_0444 family Cu/Zn efflux transporters, does contain selenoprotein examples. Intriguingly, the
398 SO_0444 family is one of only two prokaryotic transporter family we were able find previously through
399 our combination of literature review and legacy data review and validate for inclusion in reference data
400 that NCBI's Prokarotic Genome Annotation Pipeline (PGAP) uses to detect new occurrences of known
401 selenoproteins (34). The other is a small set of proteins related to the mercury resistance transporter
402 MerT. We suggest the name SaoE (SAO system metal Efflux protein) for CD2367-like proteins.
403
404 The tripeptide Cys-Ser-Cys (CSC), which is the single motif most strongly conserved between the
405 SO_0444 and SaoE families, occasionally is replaced by a selenocysteine version, Sec-Ser-Cys (USC) in the
406 SO_0444 family. Selenoprotein examples from the SO_0444 family include WP_014809615.1 from
407 *Desulfomonile tiedjei* and all of its closest homologs. We suggest that SaoE family permeases, while
408 lacking selenium in all species we examined, are involved in efflux of a potentially toxic heavy
409 metal. The absence of selenocysteine from this family means even a total lack of selenium would have
410 no effect on translation of this protein and would not block its ability to remove heavy metal (such as
411 mercury) ions from the cytosol.
412
413 Although it seems highly likely that SaoE is involved the export of either some metal-containing
414 substrate, it is unclear whether its primary physiological substrates are inorganic compounds, or
415 organometallic. The exporter SaoE is never found unless import proteins SaoP, SaoA, SaoB, and SaoX
416 also occur, suggesting the need for its metal efflux activities depends on the presence of the ABC
417 transporter.
418

419 *CD2366 family CC-COOH protein (SaoC)*
420 Homologs of CD2366 were previously protein bioinformatics "dark matter", with no available
421 crystal structure, no relevant literature detectable by PaperBLAST (27), no protein family models
422 defined by major protein family databases such as Pfam, NCBIFAMs (which includes TIGRFAMs), CDD, or
423 InterPro. PSI-BLAST searches do not reveal any homologs beyond those found in the conserved gene
424 neighborhood described in this paper. All have signal peptides, most of which appear to be lipoprotein
425 signal peptides. The average length is 158. The protein is designated SaoC (SAO system CysCys-COOH
426 protein), as nearly all end with a double-cysteine motif.
427
428 In the set of SaoC proteins from 52 representative species, just three terminate with a single Cys
429 residue instead of a CC pair. The reported coding regions for all three of these exceptional members,
430 WP_068474724.1, WP_055078435.1, and WP_070088375.1, end with a double stop codon, UGA-UAG.
431 Because the UGA codon aligns to what is otherwise an invariant Cys residue in an invariant Cys-Cys
432 motif, a selenocysteine insertion site is suspected. The 43 base nucleotide sequence starting from the
433 UGA codon of WP_055078435.1, UGAUAGUAUUUUU **UUACUUG** GGU **CAAGUAA** GGAGAGAUUAUGA,
434 shows a perfectly based paired stem of length seven (in boldface), with a G-containing loop GGU, as
435 expected for a SECIS (selenocysteine insertion sequence) element in Gram-positive species (35). Thus,
436 even in the absence of a continuation of homology C-terminal to the proposed selenocysteine, and with
437 the relatively small number of proposed selenoproteins seen in this family, we consider the confidence
438 that SaoC family proteins include selenoproteins to be high, as there is good precedence for a Cys-Sec-
439 COOH motifs in selenoproteins. Two small DUF466 family proteins are encoded in Escherichia coli K-12,
440 YbdD and YjiX, each ending Arg-Cys-Cys-COOH. Each is encoded next to a pyruvate uptake transporter,
441 either CstA or its paralog (36). A related DUF466 family selenoprotein occurs as a selenoprotein in

Campylobacter and some *Helicobacter* species, with the ending Lys-Cys-Sec-COOH (37). While the SaoC and Lys-Cys-Sec-COOH family selenoproteins exhibit no detectable homology, their shared proximity to transporters is intriguing.

SaoC family selenoproteins are the fourth set in this system with a CU motif, in addition to the permease subunit in which U is flanked by residues other than Cys, but which dimerizes so that the selenocysteine site chains of the two different monomers could be just as close. The repetition of CC and CU motifs in so many of the protein families in this nine-gene system is highly suggestive.

CD2368 family thioredoxin-like protein (SaoT)

The 61-amino acid predicted protein WP_003432954.1 from *C. difficile* is incomplete, as it is yet another selenocysteine-containing protein family. WP_012100993.1 from *Clostridium botulinum* and WP_011700724.1 from *Syntrophobacter fumaroxidans* are full-length (about 85 residues) and lack selenocysteine residues, but corrected selenoprotein sequences include WP_240067706.1 from *C. difficile*, WP_240067707.1 from *Peptacetobacter hiranonis*, and WP_240067709.1 from *Negativibacillus massiliensis*. A search with the HMM we built to detect members of this family, NF040730, detects sequence similarity, and apparent homology, to MJ0307, from *Methanococcus jannaschii,* which has a thioredoxin-like activities (38) and a solved structure (39). However, variations of the typical CXXC motif of thioredoxins and glutaredoxins that are seen in CD2368 family proteins include UPTC, CAUC, CPTC, and also CPCC. The last of these forms, CPCC, overloads the CXXC with a third Cys residue, and is the most common form across the family. By contrast, in the MJ0307-like family and among all other prokaryotic proteins in the RefSeq collection whose names contain the words “thioredoxin” or “disulfide”, a CXXC motif also never has an addition Cys in the second or third position. Less than 0.5% of CXXC motifs in such proteins have the form CCXC or CXCC. The contrast suggests that while the fold may be similar, SaoT may be undergone a change in function relative to more typical thioredoxin-like ancestral sequences, perhaps now involving direct interaction with the same family of metal-containing species as other members of the SAO system.

CD2369 family DsrE-like protein (SaoD)

Homologs of the C. difficile protein CD2369 are never detected as selenoproteins. They have an invariant CxxC motif that sometimes takes the form CxxCC, and another invariant Cys residue. The family is related to DsrE proteins identified by Pfam model PF02635, and therefore designated SaoD (SAO system DsrE-like protein). Characterized members of the DsrE family have sulfur-transfer abilities used in processes such as tRNA modification, in the cases of TusA, TusC, and TusD in E. coli, and in sulfur oxidation.

In contrast to other proteins in the SAO system, the SaoD family has a number of fairly closely related homologs found in species lacking the system, although members of the SAO system can be separated from non-members in molecular phylogenetic trees made from a multiple sequence alignment. For member proteins of the related branch found outside the set of species with the SAO system, the most frequently observed neighboring genes include homologs of metal import ABC transporter substrate-binding proteins such as AztC, metallochaperones such as AztD, and ABC transporter permease subunits for various metals. This observation further supports the notion that the SAO system interacts, at least partly, with inorganic substrates or organometallic compounds.

SaoD, like the putative organometallic lyase SaoL, is one of two proteins in the system not universally present across the 52 representative species.

489
490 **Table S1**, in Supplemental Materials, shows proteins identified by the nine new HMMs,
491 providing identities of 52 species with the conserved gene neighborhood, accession numbers for all
492 member proteins found in the SAO locus in those organism, and identities of proteins from additional
493 correlated protein families such as SelD, GrdX, and double-cubane proteins identified by phylogenetic
494 profiling and gene neighborhood analyses.

495 *Partial Phylogenetic Profiling results.*
496 A phylogenetic profile was constructed by use of the new NCBIFAMs model NF040734, which
497 finds members of the SaoC family of CysCys-COOH proteins. The profile included 33 YES genomes, from
498 3217 genomes in the PPP genomes, for a probability *p* of about 0.01. PPP was run with the YES
499 frequency parameter elevated to the manually set value of 0.03. Increasing this parameter, used in
500 binomial distribution computations by PPP, compensates for an intrinsic bias problem in comparative
501 genomics studies from the fact that species from the same lineage share larger numbers of closely
502 related protein pairs, simply because of recent common ancestry.
503
504 Partial Phylogenetic Profiling (PPP) studies were performed on the proteomes of assemblies
505 GCF_000009205.1 (*Clostridioides difficile*), GCF_000014965.1 (*Syntrophobacter fumaroxidans*),
506 GCF_000325665.1 (*Brachyspira pilosicoli*), GCF_001754075.1 (*Merdimonas faecis*), and
507 GCF_001940565.1 (*Tissierella creatinophila*). **Table S2** in Supplementary materials lists the 40 top-
508 scoring proteins from each of five species, showing the PPP score, RefSeq protein accession number, and
509 functional name. All sets of results showed members of the SAO system's nine core protein families of
510 this system as the top-scoring proteins, although with gaps occurring for those proteins where previous
511 treatment of selenocysteine-encoding TGA codons as stop codons blocked proper structural
512 annotation. The high scores from PPP reflected not only that these proteins were all universal across
513 species with the system (within the limits of structural annotation accuracy at the time the PPP data set
514 was built), but also that strong BLAST score matches to proteins in these families do not occur to
515 proteins in genomes lacking the system.
516
517 All proteins with PPP scores higher than 50 (that is, with computed odds of such a high
518 rate of co-occurrence just by chance being 1e-50 or less) from any of the five genomes belongs to the
519 SAO locus. That is, we detected no additional components of the SAO system outside the set of nine
520 proteins families described. High scores were achieved for these because all homologs in the PPP
521 reference set were being found in species with the marker SaoC. Example scores in *C. difficile* include
522 115.7 for WP_070088344.1 (SaoC itself, hitting 33 YES genomes in the top 33 hits), 107.2 for
523 WP_009897547.1 (SaoB fragment C-terminal to the selenocysteine, with 30 YES genomes out of 30 hit),
524 and 53.3 for WP_004454661.1 (SaoB fragment N-terminal to the selenocysteine. 16 YES genomes from
525 the top 17 hits).
526
527 The next tier, all scoring below 40, includes proteins such as WP_084191679.1 from *Tissierella*
528 *creatinophila*, a glycine reductase complex selenoprotein B (GrdB). The top 148 sequences hit occur in
529 144 different genomes, including 27 that have the SAO system, for a score of 37.1. Proteins appearing
530 in this tier can include both those with direct connections, as when the end product of one pathway is a
531 substrate for another, and those frequently co-occuring because of sharing biological similarities such
532 niche and ancestry. GrdB may be correlated because 1) its species distribution, though broad, skews
533 strongly toward the taxonomic class *Clostridia*, 2) it functions only in anaerobic environments, just as
534 the SAO system seems to, and 3) it requires a selenium insertion proteins SelA, SelB, and SelD. For

535 similar reasons, proteins associated with selenium-dependent molybdopterin hydroxylases occur in this
536 second tier, including predicted selenium cofactor biosynthesis proteins YqeB and YqeC (6,7).
537
538 *Associated Double-Cubane proteins*.
539 Supplemental file **SAO_system_PPP_top_hits.xlsx**, in supplemental materials, shows the top 40
540 hits from PPP for five phylogetically diverse species: *Brachyspira pilosicoli, Clostridioides difficile,*
541 *Merdimonas faecisa, Syntrophobacter fumaroxidansa,* and *Tissierella creatinophila*. The surprise family
542 of protein at the top of the second tier of PPP scores is the family of 8Fe-9S cofactor-containing "double-
543 cubane" proteins. As can be seen for all five species, at least one of the top five proteins is a double-
544 cubane protein. That includes two species in which it is the top such hit, and two more where it is
545 second. In double-cubane enzymes, two 4Fe-4S iron-sulfur clusters make contact through an additional
546 bridging sulfur atom, creating an unusual 8Fe-9S metallocenter (40,41). The side chains of seven
547 conserved Cys residues, forming the motif 7-Cys motif CX(19)CX(18-19)CX(29)CX(166-170)CX(32-
548 34)CX(32)C, provide ligands to the cluster. These proteins are not known to have a connection to
549 selenium metabolism. 8Fe-9S-type double-cubane proteins are described as having the ability to
550 reduce refractory small molecules such as acetylene and hydrazine (40), but in general, physiologically
551 relevant substrates are not known. Their closest homologs among more completely characterized
552 proteins include beta subunits of enzymes such as (R)-phenyllactyl-CoA dehydratase, (R)-2-
553 hydroxyisocaproyl-CoA dehydratase, and (R)-2-hydroxyglutaryl-CoA dehydratase. These enzymes
554 require an ATP-hydrolyzing activase, an extremely oxygen-sensitive enzyme that transfers a single
555 electron to its target, after which the dehydratase can perform large numbers of turnovers (42).
556
557 We built a new HMM, accession number NF040772, to describe double-cubane cluster-
558 containing putative anaerobic reductases. Most were annotated, at the beginning of this study, as "2-
559 hydroxyacyl-CoA dehydratase" or as "2-hydroxyacyl-CoA dehydratase family protein." Of the 15,511
560 genomes in the calibration set, just 735 genomes (4.7 %) have a double-cubane protein as detected by
561 hidden Markov model NF040730. But quite remarkably, 11.8 % of all double-cubane proteins occur in
562 the 0.3 % of representative genomes that have the SAO system. Among genomes with at least one
563 double-cubane protein, the count per genome is higher in species with the SAO cassette (2.2 per
564 genome) than in species without (1.2 per genome). Among the 52 species with SAO cassette, 21 (40%)
565 have at least one double-cubane protein encoded within 5000 nucleotides of the cassette, and often
566 more than one. Examples of genomes with double-cubane proteins next to the SAO cassette are
567 *Clostridium botulinum* (see Figure 4), *Clostridium sporogenes, Desulfopila aestuarii, Gottschalkia*
568 *purinilytica,* and *Syntrophorhabdus aromaticivorans.*
569
570 The NF040772 family of double-cubane enzymes includes many examples from genomes that
571 lack the SAO system, including the uncharacterized enzyme YjiM from *Escherichia coli* K-12. However,
572 we were unable to find sequence signatures we could use to separate double-cubane from genomes
573 with the SAO system from their counterparts in genomes without. The comparative genomics therefore
574 seems to suggest the SAO system requires the presence of at least one double-cubane protein, but not
575 the other way around. Substances becoming available in the cytosol as a consequence of the SAO
576 system may enter a pool of compounds that double-cubane proteins can act on, and not be chemically
577 distinguishable from substrates obtained in other ways.
578
579 *Double-cubane proteins and selenium*
580 Every species with SAO system has both selenocysteine and one or more members of the
581 NF040772 branch of the family of double-cubane proteins. We therefore looked at the relationship
582 between those double-cubane proteins and selenium. SelD is the selenophosphate biosynthesis enzyme

583 needed for selenocysteine, selenouridine, and selenium-molybdenum cofactor biosynthesis. It is more
584 common in anaerobes than aerobes, and is found in just 38 percent of representative genomes overall.
585 However, 955 of 970 of double-cubane proteins that score > 400 bits to hidden Markov model
586 NF040772 are encoded in SelD-containing assemblies. Of the 15 exceptions, three are from bacteria
587 that encode selenocysteine biosynthesis protein SelA, suggesting that SelD's apparent absence may be
588 artifactual, and nine others are from methanogenic archaea. Of over 900 examples of bacterial double-
589 cubane proteins identified in representative assemblies, only three are from assemblies lacking SelD.
590
591 This remarkably close association of the NF040772 and SelD families could be explained by a
592 role for double-cubane enzyme in processing selenium-containing compounds, or in pathways that have
593 obligatory selenium-dependent steps either before or after. Explanations of this kind for the double-
594 cubane enzyme to selenium linkage are plausible and may be seen as more likely than a previously
595 unsuspected novel chemistry. But we list as a formal possibility the explanation that the structure of the
596 cofactor itself is what links the selenium donor protein SelD to the NF040772 family of double-cubane
597 proteins. The correlation we detect may signify biosynthesis of selenium-bridged analogs of the recently
598 described 8Fe-9S cofactor in a subset of double-cubane proteins. If so, then the active site cluster in
599 double-cubane proteins and selenocysteine sidechains in SAO system proteins may share abilities to
600 bind a similar class of compound through a selenium atom. The product or an intermediate of one
601 system may be a substrate acted upon by the other.
602
603 *Revisiting methylmercury formation proteins HgcA and HgcB*.
604 Proteins DND132_1056 (EGB14269.1) and DND132_1057 (EGB14270.1) in *Desulfovibrio*
605 *desulfuricans* ND132, and similar pair GSU1440 (AAR34814.1) and GSU1441 in *Geobacter sulfurreducens*
606 PCA, were described in by Parks, et al. in 2013 as proteins HgcA and HgcB of a two protein cluster
607 needed for methylmercury formation (43).
608
609 Unlike DND132_1056 and GSU1440, the founding members of HgcA family described by Parks,
610 et al., occasional homologs differ by having N-terminal extensions that include CC motifs. One such
611 proteins was examined in a site-directed mutagenesis study (44). We examined the coding capacity of
612 5'-extended versions of the coding region for DND132_1056, GSU1440, and 18 additional homologs of
613 similar length. In all 20 cases, we found that the coding region could be extended upstream, to a new
614 length between 363 and 400 amino acids, by allowing translation of a single UGA codon as
615 selenocysteine. The minimal required N-terminal extensions are
616 MAPPDVPARDDAPC**U**GPRPDPRAGVFEKPGYAVEPFV for DND132_1056, and
617 MSQPGPDVDRPPC**U**GPKTPAVSGTINENVPGFLRWLDTPAGR for GSU1440. Across all 20 proteins, the
618 pentapeptide motif surrounding the selenocysteine residue is perfectly conserved, PCUGP, and all
619 species encode the proteins required for selenocysteine incorporation. The CU motif resembles that
620 from several selenoproteins of the SAO system, and lends further support to the notion that the SAO
621 might be involved in organometallic compound formation, as well as dismutation.
622
623 Examination of HgcB showed that it too contains selenoproteins, 17 of 266 examples (6.4%).
624 While the HgcB , like SaoC, has a Cys-Cys dipeptide as the final two residues for nearly every family
625 member, the site of selenocysteine incorporation in HgcB differs, occurring instead about 25 amino
626 acids from the C-terminus, at residue 73, the 9th of HgcB's invariant Cys residue positions.
627
628 **Figure 5** shows the similarity CU motifs found in this study for in several key proteins of the SAO
629 locus and in methylmercury formation protein HgcA. The CU motif is relatively rare in selenoproteins.
630 We see it in the uncharacterized CUAEP/CCAEP-tail radical SAM protein (NF040546) and at the C-

631 terminus of the Campylobacter/Helicobacter lineage KCU-star (NF033934), both of whose structures and
632 functions are not well known. It occurs in a small group of mercuric transporter MerT family
633 selenoproteins such as WP_250634603.1, and in redoxin domain-containing proteins in the family
634 related to WP_012872293.1, but in no other selenoprotein we know of outside of the SAO and HgcAB
635 systems. We find the three examples in SAO system remarkable, and the sharing of the CU motif with
636 HgcA proteins to be highly suggestive of a shared interaction with a heavy metal atom. The CU in the
637 SAO system occurs in protein exposed to the extracellular milieu (SaoC and SaoB), but also in the cytosol
638 (SaoL). We can add to this SaoT, a thioredoxin-like protein, which has two different forms of
639 selenocysteine-containing motifs, UXXC and CXUC, in addition to two non-selenoprotein forms, and
640 cysteine-overload CXCC form (extremely rare in other thioredoxin like proteins) and the CXXC form
641 expected in thioredoxins. It seems quite likely that the multiple selenoproteins of the SAO system, or
642 their Cys-overloaded non-selenoprotein homologs, bind a mercury-like heavy metal-containing part of
643 some compound, or class of compound, as it is trafficked from outside the cell to inside, most likely
644 undergoing covalent changes in the process. While possible roles for the SAO system could include
645 making mercury less toxic for itself, or more toxic for competing organisms, we speculate that an
646 alternative role could be the catalytic use of a trace element present in extremely small quantities for sa
647 new type of selenium-assisted energy metabolism.
648
649 *Rolling reannotation of RefSeq genomes*
650 RefSeq regularly subjects prokaryotic assemblies to reannotation by the PGAP prokaryotic
651 genome annotation pipeline (19) so that both structural and functional annotation can be kept up-to-
652 date. Reference data that enables proper prediction of all novel selenoproteins described in this paper
653 has been added to PGAP, so the rolling reannotation is replacing fragmented, incomplete, or missing
654 selenoproteins with corrected versions containing U, the single letter code for selenocysteine, in the
655 amino acid sequence. The exception is SaoC, as PGAP currently cannot correctly predict C-terminal
656 selenocysteine residues. Sequences belonging to any of the HMM-defined protein families listed in
657 Table 1 and currently annotated on any RefSeq genome can be retrieved by query with the HMM's
658 accession number at https://www.ncbi.nlm.nih.gov/protfam. Genomic regions that now have correctly
659 annotated selenoproteins can be visualized, such as
660 https://www.ncbi.nlm.nih.gov/nuccore/NZ_CP046450.1?report=graph&from=2931388&to=2941900, as
661 seen in Figure 4, or
662 https://www.ncbi.nlm.nih.gov/nuccore/NZ_JAGIVI010000014.1?report=graph&from=60051&to=66700
663 &strand=true for a *Clostridioides difficile* strain JV65 033.
664
665 Figures S1 through S8 in supplemental materials show full-length or minimally trimmed
666 alignments for the eight selenoprotein-containing families discussed in this paper. Sequences in each
667 alignment were made non-redundant by removing the shorter protein from any pair above a certain
668 percent identity. These thresholds were 80% for SaoL (Figure S1), SaoB (Figure S2), SaoP (figure S3), and
669 SaoT (figure S4). The thresholds used were 85% for SaoX (Figure S5), 95% for SaoC (figure S6), and 90%
670 for HgaB (figure S8), families in which selenoproteins are relatively rare. The alignment for HgcA (figure
671 S7) shows selected sequences from the family, non-redundant to below 75% identity, with some manual
672 editing to correct small errors made during progressive alignment by Clustal W. Alignments for SaoL,
673 SaoB, SaoP, SaoT, HgcB, but not SaoC, SaoX, or HgcA, include sequences that have not yet reached by
674 RefSeq's rolling reannotation and that therefore appear in truncated form, either N-terminally or C-
675 terminally, caused by improper treatment of the selenocysteine-encoding UGA codon as a stop codon.
676
677
678 **Discussion:**

679 *The SAO system contains six novel selenoprotein families*
680 We have described here a rare but taxonomically diverse conserved gene neighborhood that is
681 exceptional in a number of ways. In a collection of representative prokaryotic genomes, one per species
682 for 15,511 species, the system occurs in just 52 genomes, broadly distributed taxonomically, but focused
683 on anaerobes that show various adaptations for performing biochemically challenging fermentations in
684 anaerobic environments. The system is a nine-gene operon, encoding four previously unknown protein
685 families that are selenocysteine-containing a majority of the time (98%, 85%, 65%, and 60% for SaoL,
686 SaoP, SaoT, and SaoB, respectively). Two additional families contain small numbers of selenoproteins,
687 bringing the set of novel selenoproteins up to six new families.
688
689 *CC and CU motifs suggest interaction with heavy metal atoms.*
690 The putative organometallic lyase SaoL has a CU motif that aligns to a mercury-binding Cys at
691 MerB's active site. The putative metal efflux transporter SaoE has a CSC motif that aligns to the motif
692 USC in selenoprotein homologs in the SO_0444 family of Cu/Zn efflux transporters. Additional signature
693 motifs in the SAO system include CU in the predicted substrate-binding pocket of SaoB, CC in the
694 substrate-binding cleft of SaoX, U at the gating position of the homodimer-forming permease SaoP,
695 CXUC and variations at the redox disulfide bond-like site in SaoT, and a C-terminal CC motif that
696 sometimes is CU in the dark matter protein SaoC. This is a remarkable repetition of the selenocysteine
697 or double-cysteine theme across the SAO, within each system suggesting multiple proteins interacting
698 with the same metal or its adducts at multiple cellular sites.
699
700 *Selenocysteine is unknown in characterized mercury resistance protein families, but is discovered in*
701 *methylmercury formation*
702 Our previous extensive efforts to catalog authenticated prokaryotic selenoproteins as structural
703 reference sequences for NCBI's PGAP prokaryotic genome annotation pipeline resulted in no examples
704 of a selenoprotein involved in mercury resistance. This made us curious about the need for
705 selenocysteine in the MerB homolog SaoL and in the rest of the SAO operon. Our suspicion that the
706 system might catalyze for the formation and the dismutation of organometallic compounds sparked our
707 interest in a previously described pair of proteins known to participate in organomercurial compound
708 formation, HgcA and HgcB. Examination of the HgcA and HgcB proteins revealed that both can be
709 selenoproteins, HgcA in the great majority of cases, with a previously unknown N-terminal extension,
710 and HgcB occasionally. The motifs are CU in the newly discovered N-terminal extension of HgcA
711 selenoproteins for methylmercury formation, and CC at the C-terminus of HgcB, echoing what is seen in
712 the SAO system. We found these strong parallels between the SAO and HgcAB systems, in the use of
713 selenocysteine and the prevalence of CU and CC motifs, only after we started to hypothesize that the
714 SAO system could form organometallic compounds as pathway intermediates, and consider our
715 observations about selenocysteine's role in methylmercury formation to be significant support.
716
717 *Co-occurring proteins suggest adaptation to anaerobic environments by selenocysteine-enabled*
718 *fermentation of normally refractory substrates.*
719 We described above a special relationship between the SAO system and 8Fe-9S cofactor-
720 containing double-cubane proteins, showing that double-cubane proteins are universally present in
721 SAO-containing genomes, extra abundant in those genomes, and encoded adjacent to SAO proteins in
722 almost half of those genomes. Correlations with *grd* (Glycine Reductase) genes are similarly
723 informative. These genes of Stickland metabolism include grdB (glycine reductase complex
724 selenoprotein B), grdH (betaine reductase selenoprotein B), and grdF (sarcosine reductase complex
725 component B subunit beta) all are selenoproteins that help enable anaerobic fermentations most
726 bacteria cannot do. In Stickland fermentations, oxidation of one amino acid is coupled to reduction of

727 another (or of sarcosine or betaine). The reductive metabolism leads to ATP formation (45). SAO
728 operons are present in 0.3% of bacterial species, but in 13.4% of those with GrdX family proteins. GrdX
729 is present in just 2.2% of genomes, but in 87% of those with SAO. Both SAO and Stickland metabolism
730 require selenocysteine, but selenoprotein families involved in processes other than Stickland
731 metabolism do not show such strong patterns of co-occurrence with SAO. For example, Clostridium
732 difficile has a selenocysteine-containing formate dehydrogenase, but its Partial Phylogenetic Profiling
733 score does not place it in the 1500 proteins best correlated with the SAO system.
734
735 *The SAO system's conservation, context, and patterns of design suggest metabolism, not resistance*
736 The SAO system is sporadically distributed, as are the markers of Stickland fermentation, found
737 in bacteria that are taxonomically highly divergent, while occupying similarly anaerobic environments.
738 Examples of the operon we have viewed in extended local context show no signs of inhabiting mobile
739 islands now or having undergone recent horizontal gene transfer. All genomic contexts we viewed
740 showed housekeeping-type genes as neighbors rather than apparent markers of mobility such as
741 transposases or phage or plasmid proteins.
742
743 Conservation within lineages similarly suggests a central metabolic role. The *C. difficile* genome
744 is known to be heavily invaded by mobile elements and mosaic in structure (46), so substantial
745 variability of genome content is expected from one strain to another. Genes that help confer resistance
746 to trace metals such as mercury or arsenic, such as *merA*, typically frequently appear in plasmids, or in
747 genomic islands flanked by markers of mobility. We find *merA*, encoding mercury(II) reductase, in 5469
748 of 34051 RefSeq assemblies (16%) of *Escherichia coli*. By contrast, we find the SAO system in *C. difficile*
749 in 3279 of 3343 assemblies (98%). All genomic contexts we viewed showed housekeeping-type genes as
750 neighbors rather than apparent markers of mobility such as transposases or phage or plasmid proteins.
751
752 The SAO system's *pattern of design* (47) seems to argue against a resistance function, and
753 therefore to further support a metabolic role such as energy metabolism. The system occurs exclusively
754 in bacteria that grow anaerobically, and mostly in members of the Firmicutes, bacteria that lack an outer
755 membrane. The MerT and MerP proteins in Gram-negative transport the highly toxic mercuric ion,
756 Hg(II), from the periplasmic space to the cytosol, where MerA can convert it to the less toxic Hg atom.
757 But for species that lack an outer membrane to enclose a periplasmic space, it seems an unfavorable
758 design to import mercury ions or compounds from the whole of the extracellular milieu in order to
759 detoxify them, imposing energy costs for substrate import, metal efflux, and expression of nine different
760 proteins. Similarly, relying on selenoproteins seems like a strange design with and inherent liability if the
761 purpose of the SAO system is mercury resistance. A lack of selenium would block protein translation and
762 prevent the function of proteins needed for resistance if selenium is in short supply. Having such
763 limitation is plausible, of course, but we have encountered no examples.
764
765
766 *Catalysis vs. binding affinity.*
767 Selenocysteine in prokaryotes is well known for replacing Cys in enzymes at the active site,
768 giving the enzyme dramatically higher catalytic efficiency than its Cys analog would have. Selenocysteine
769 is far less common in proteins without enzymatic or redox function. But selenoproteins SaoB and SaoP
770 are binding and permease subunits of an ABC transporter, normally expected to have a binding but not a
771 catalytic role. Their selenocysteine sidechains raise the prospect of a dual role for the transporter.
772 Selenium atoms in contact with the transporter's substrate might effect some covalent change. Two
773 different SBPs work together with a single permease that has a pair of active site-like selenocysteine
774 sidechains meeting at the crystallography-defined substrate-gating site. Any number of different

775 scenarios could be proposed in which the SAO system's ABC transporter assembles a substrate molecule
776 before transporting it. Catalysis by transporters has ample precedent, including sugar import tied to
777 phosphorylation in PTS transporters. On the other hand, there is an extraordinarily high binding affinity
778 between selenium and mercury (48). Multiple steps in the handling of a single substrate found in the
779 extracellular milieu, involving binding rather than catalysis, could be the reason so many selenoproteins
780 are found in the SAO system.
781
782 *Is mercury itself the most likely metal for the SAO system to traffic?*
783 Multiple lines of evidence suggest the binding to, transport of, and likely the formation and/or
784 dismutation of organometallic compounds. But is not clear that mercury is the only or even principal
785 metal involved. MerB family lyases are known to accommodate metals other than mercury at the
786 mercury-binding site, even if physiological substrates other than organomercurial compounds are not
787 known. The CU motif at the heavy metal binding site of SaoL is non-canonical for the MerB family, so it
788 cannot be assumed automatically that organomercurials are appropriate substrates.
789
790 Most components of the SAO system are invariably present, but SaoL itself occasionally is not
791 detected, missing in 9 of 52 loci. How the system could include in most cases such a vividly suggestive
792 component, yet dispense with it in some bacteria, is unclear. But these variant forms of the system may
793 provide some clues to the function of the system. *Desulfopila aestuarii* has a replacement for SaoL, an
794 apparently authentic MerB protein, WP_073613903, encoded in the middle of the SAO operon. This
795 replacement protein has much higher levels of sequence identity to homologs found in the middle of
796 mercury resistance loci than it does to any SaoL protein.
797
798 Our best guess for the reason that SaoL can be dispensable is that the system can act on a
799 variety of metals, and the system may not require Hg to be present. We have suggested that
800 organometallic compounds are formed for transient existence, as they would be consumed later in a
801 pathway that is part of fermentation for energy generation. The organic portion of the molecule may
802 undergo redox changes, with the attached metal atom facilitating otherwise biochemically difficult
803 transformations. The final step, liberating the metal moiety from the fully reduced end product, might
804 proceed non-enzymatically at a sufficient rate, for metals other than mercury, that SaoL is not required.
805
806 *Model for the biological process carried by proteins of the SAO system.*
807
808 We suggest that the selenoprotein-loaded SAO system provides a novel mechanism for *C.*
809 *difficile*, and other bacteria that share the same rare operon, to make use of certain normally refractory
810 organic substrates in organically rich but oxidant-poor environments. More specifically, we suggest that
811 the SAO system manages the import of a food source that most bacteria cannot readily utilize in
812 anaerobic conditions, and furthermore, that at some point during the process of import and catabolism,
813 enzymes and/or transporters are acting on an organometallic compound. Said organometallic
814 compound might typically have a short half-life in solution, but is chaperoned before, during, and after
815 transport by selenoproteins that have multiple Cys or Sec residues in contact with the metal atom.
816 Following import, the compound is reduced by an 8Fe-9S (or possibly a 2(4Fe-4S)-Se) cluster-containing
817 double-cubane protein, making the compound an oxidant that enables ATP generation by other cellular
818 machinery, such as the energy-transducing Rnf complex (45). Once the compound can no longer be
819 reduced further, the carbon-metal bond may be cleaved by SaoL, chaperoned to the efflux transporter
820 SaoE, and extruded. It is further possible that the metal, when extruded, is captured for reuse in the
821 next turn of the cycle. In this scenario, even trace amounts of a heavy metal with the right properties

822 could serve a catalytic role to provide a competitive advantage in energy metabolism to bacteria with
823 the SAO system.
824
825 Although our model is admittedly highly speculative, it is built on a number of potentially
826 important underlying observations about various protein families and their unexpected structures and
827 relationships. Quite a number of experiments to confirm or falsify part of the model immediately
828 suggest themselves, including tests for uptake of and sensitivity to mercury and other heavy metals,
829 ability to metabolize various compounds with or without certain metals present, ability to form or
830 cleave various organomercurial compounds, and how these results change if certain genes within the
831 SAO system are knocked out.
832
833 Our discovery of eight novel selenoprotein families overall, six in the SAO system and two in
834 methylmercury biosynthesis, suggests there may be many others left to find, with potential importance
835 in understanding conversions of heavy metals to more or less toxic forms in gut or environmental
836 microbiomes, or for bioengineering applications. We suggest that selenocysteine side chains may
837 potentiate organometallic compound biosynthesis in a wide variety of individually rare pathways that
838 remain to be discovered. Their relative rarity, plus the likely scarcity of non-selenoprotein homologs to
839 assist with their discovery, has likely made such systems difficult to discover in the past. However, the
840 potential for finding more such systems now seems clear. Families of novel organometallics may have
841 transient existences in anaerobic metabolism as pathway intermediates, including in gut microbiomes,
842 undergoing formation, transport, transformation, and dismutation, all in pathways that remain to be
843 discovered, in part because key markers of those systems are still-undiscovered selenoproteins.
844
845 *This research was supported by the Intramural Research Program of the National Library of Medicine at*
846 *the NIH. This work utilized the computational resources of the NIH HPC Biowulf cluster*
847 *(http://hpc.nih.gov). The authors would like to thank Eric Boyd and Ian Krout for helpful discussions.*
848
849
850 Table 1.

Protein Accession	HMM	gene	provisional protein name	U/C+U
WP_012048219	NF040730	saoT	thioredoxin-like protein SaoT	34/52
WP_012048218	NF040736	saoE	ArsP-related export pemease	0/52
WP_003357554	NF040734	saoC	Cys-Cys-COOH protein SaoC	3/52
WP_012048217	NF040735	saoX	ABC transporter substrate-binding protein SaoX	2/53
WP_240004094	NF040728	saoL	MerB-related organometallo-lyase SaoL	44/45
WP_242649186	NF040727	saoB	ABC transporter substrate-binding protein SaoB	31/52
WP_242649185	NF040733	saoP	ABC transporter permease subunit SaoP	44/52
WP_012048215	NF040729	saoA	ABC transporter ATP-binding subunit SaoA	0/52
WP_003357559	NF040732	saoD	DsrE-related protein SaoD	0/35

851
852
853 Figure Legends:
854
855 **Figure 1**: AlphaFold2 structure of $SaoM_{Cdiff}$Sec162Cys with structural alignment to MerB structure 3F0P.
856 The left panel shows alignment of the complete structures, with SaoM rainbow-colored from N-
857 terminus (red) to C-terminus (purple), while MerB is colored gray. The right panel shows closeups of the

858 Hg atom bound by MerB from the same superposition of structures. In this panel, MerB and the Hg
859 atom are gray, while $SaoM_{Cdiff}$Sec162Cys is colored by AlphaFold2 pLDDT scores of local structural
860 prediction confidence (see key). SaoM residues Cys99, Asp102, and Sec162Cys (indicated by arrows)
861 align to MerB's active site residues Cys96, Asp99, and Cys159.
862
863
864 **Figure 2**: AlphaFold2 prediction for $SaoP_{Cdiff}$Sec210Cys as a homodimer and structural alignment to
865 structure 3HDW for the Escherichia coli ABC transporter permease subunit MetI in the open-inwards
866 conformation. The left panel shows a side view, with the bottom facing the cytosol. The right panel
867 shows a view of homodimeric $SaoP_{Cdiff}$Sec210Cys as seen top-down from outside the plasma membrane
868 after rotation 90^0. Amino acid side chains are shown only for the Cys residue that represents Sec210,
869 which occupies that same position in the center of the image as the permease-gating residue Met-163 in
870 the MetI solved structure.
871
872
873 **Figure 3**. AlphaFold2 predicted structures for putative ABC transporter organometallic substrate-
874 binding proteins SaoB and SaoX. Coloring reflects the pLDDT metric of confidence in the local structure.
875 The left panel shows a prediction based on *C. difficile*'s SaoB selenoprotein WP_239591066.1, after
876 trimming an N-terminal signal sequence and replacing Sec72 with Cys. Locations are shown for Cys/Sec
877 residues conserved across the SaoB family, found at positions 71, 72, and 91. All S/Se atoms are near
878 each other and may help form a metal-binding site in a substrate-binding pocket or cleft. A fourth Cys
879 residue is not shown because it is not well conserved in a multiple alignment of SaoB sequences. The
880 right panel shows the lipoprotein SaoX of *C. difficile*, WP_004454662.1, after trimming the predicted
881 lipoprotein signal peptide. An additional N-terminal region is predicted with low confidence (reddish-
882 orange color) and not made part of the globular structure. The rest packs in a structure highly similar to
883 ABC transporter substrate-binding protein PDB structures, such as 4NMY and 2X26. Four conserved Cys
884 residues are found at positions 50, 192, 224, and 225, and their side chains conserve to form what again
885 appears to be a metal-binding site. In about 40% of SaoX proteins, the residue preceding Cys-192 is
886 cysteine as well, forming a CC motif.
887
888
889 **Figure 4:** PGAP annotation of the 9-gene *sao* (Selenocysteine-Assisted Organometallic) operon and
890 adjoining double-cubane locus in *Clostridium botulinum* strain NCTC 13319. The region shown is from
891 RefSeq nucleotide sequence NZ_CP046450.1 (2931388-2941900). The SAO (selenocysteine-assisted
892 organometallic) locus (yellow box) gene order is *saoTECXLBPAD*. Black vertical arrows show
893 selenocysteine (Sec) insertion codons in *C. botulinum*. Short green vertical arrows show locations where
894 Sec occurs in orthologs from other species. C. botulinum was selected from among 21 *sao* locus-
895 containing representatives with nearby double cubane proteins and their activase (gray box). A
896 comparable re-annotated *sao* region in *C. difficile,* NZ_JAGIVI010000014.1(60051-66700), has four
897 selenoproteins instead of three, with the genes in a different order, *saoDTECXBPAL* (not shown). The
898 lone 8Fe-9S double-cubane protein in that genome, WP_004454390, is located more than 500,000 base
899 pairs away.
900
901 **Figure 5**: Alignments of selenoprotein and non-selenoprotein versions of proteins SaoL (top left), SaoB
902 (top right), SaoC (bottom left), and HgcA (bottom right), for short regions that include the site where the
903 selenocysteine may occur, are show as displayed in belvu (16), colored by residue type. For SaoL,
904 homolog of the organomercurial lysase MerB, the top sequence (WP_087258257.1) was exceptional for
905 having Cys (C) rather than Sec (U), and the site is "packed", with four consecutive Cys residues. Similar

packing with extra Cys residues is seen in methyl mercury formation protein HgcA region. Full-length multiple sequence alignments for all eight selenoprotein families described in this paper can be found in Supplemental Materials.

1. Neumann-Schaal, M., Jahn, D. and Schmidt-Hohagen, K. (2019) Metabolism the Difficile Way: The Key to the Success of the Pathogen Clostridioides difficile. *Front Microbiol*, **10**, 219.
2. Gencic, S. and Grahame, D.A. (2020) Diverse Energy-Conserving Pathways in Clostridium difficile: Growth in the Absence of Amino Acid Stickland Acceptors and the Role of the Wood-Ljungdahl Pathway. *J Bacteriol*, **202**.
3. Hryckowian, A.J., Pruss, K.M. and Sonnenburg, J.L. (2017) The emerging metabolic view of Clostridium difficile pathogenesis. *Curr Opin Microbiol*, **35**, 42-47.
4. Jackson, S., Calos, M., Myers, A. and Self, W.T. (2006) Analysis of proline reduction in the nosocomial pathogen Clostridium difficile. *J Bacteriol*, **188**, 8487-8495.
5. Peng, T., Lin, J., Xu, Y.Z. and Zhang, Y. (2016) Comparative genomics reveals new evolutionary and ecological patterns of selenium utilization in bacteria. *ISME J*, **10**, 2048-2059.
6. Haft, D.H. and Self, W.T. (2008) Orphan SelD proteins and selenium-dependent molybdenum hydroxylases. *Biol Direct*, **3**, 4.
7. Zhang, Y., Turanov, A.A., Hatfield, D.L. and Gladyshev, V.N. (2008) In silico identification of genes involved in selenium metabolism: evidence for a third selenium utilization trait. *BMC Genomics*, **9**, 251.
8. Gladyshev, V.N., Khangulov, S.V. and Stadtman, T.C. (1996) Properties of the selenium- and molybdenum-containing nicotinic acid hydroxylase from Clostridium barkeri. *Biochemistry*, **35**, 212-223.
9. Self, W.T., Wolfe, M.D. and Stadtman, T.C. (2003) Cofactor determination and spectroscopic characterization of the selenium-dependent purine hydroxylase from Clostridium purinolyticum. *Biochemistry*, **42**, 11382-11390.
10. Srivastava, M., Mallard, C., Barke, T., Hancock, L.E. and Self, W.T. (2011) A selenium-dependent xanthine dehydrogenase triggers biofilm proliferation in Enterococcus faecalis through oxidant production. *J Bacteriol*, **193**, 1643-1652.
11. Zhang, Y., Romero, H., Salinas, G. and Gladyshev, V.N. (2006) Dynamic evolution of selenocysteine utilization in bacteria: a balance between selenoprotein loss and evolution of selenocysteine from redox active cysteine residues. *Genome Biol*, **7**, R94.
12. Altschul, S.F., Madden, T.L., Schaffer, A.A., Zhang, J., Zhang, Z., Miller, W. and Lipman, D.J. (1997) Gapped BLAST and PSI-BLAST: a new generation of protein database search programs. *Nucleic Acids Res*, **25**, 3389-3402.
13. Eddy, S.R. (2009) A new generation of homology search tools based on probabilistic inference. *Genome Inform*, **23**, 205-211.
14. Thompson, J.D., Higgins, D.G. and Gibson, T.J. (1994) CLUSTAL W: improving the sensitivity of progressive multiple sequence alignment through sequence weighting,

950 position-specific gap penalties and weight matrix choice. *Nucleic Acids Res*, **22**, 4673-
951 4680.
952 15. Edgar, R.C. (2004) MUSCLE: multiple sequence alignment with high accuracy and high
953 throughput. *Nucleic Acids Res*, **32**, 1792-1797.
954 16. Sonnhammer, E.L. and Hollich, V. (2005) Scoredist: a simple and robust protein
955 sequence distance estimator. *BMC Bioinformatics*, **6**, 108.
956 17. Sonnhammer, E.L. and Durbin, R. (1995) A dot-matrix program with dynamic threshold
957 control suited for genomic DNA and protein sequence analysis. *Gene*, **167**, GC1-10.
958 18. Mariotti, M., Lobanov, A.V., Guigo, R. and Gladyshev, V.N. (2013) SECISearch3 and
959 Seblastian: new tools for prediction of SECIS elements and selenoproteins. *Nucleic Acids*
960 *Res*, **41**, e149.
961 19. Li, W., O'Neill, K.R., Haft, D.H., DiCuccio, M., Chetvernin, V., Badretdin, A., Coulouris, G.,
962 Chitsaz, F., Derbyshire, M.K., Durkin, A.S. *et al.* (2021) RefSeq: expanding the Prokaryotic
963 Genome Annotation Pipeline reach with protein family model curation. *Nucleic Acids*
964 *Res*, **49**, D1020-D1028.
965 20. Basu, M.K., Selengut, J.D. and Haft, D.H. (2011) ProPhylo: partial phylogenetic profiling
966 to guide protein family construction and assignment of biological process. *BMC*
967 *Bioinformatics*, **12**, 434.
968 21. Haft, D.H., Paulsen, I.T., Ward, N. and Selengut, J.D. (2006) Exopolysaccharide-
969 associated protein sorting in environmental organisms: the PEP-CTERM/EpsH system.
970 Application of a novel phylogenetic profiling heuristic. *BMC Biol*, **4**, 29.
971 22. Gibrat, J.F., Madej, T. and Bryant, S.H. (1996) Surprising similarities in structure
972 comparison. *Curr Opin Struct Biol*, **6**, 377-385.
973 23. Wang, J., Youkharibache, P., Marchler-Bauer, A., Lanczycki, C., Zhang, D., Lu, S., Madej,
974 T., Marchler, G.H., Cheng, T., Chong, L.C. *et al.* (2022) iCn3D: From Web-Based 3D
975 Viewer to Structural Analysis Tool in Batch Mode. *Front Mol Biosci*, **9**, 831740.
976 24. Wang, J., Youkharibache, P., Zhang, D., Lanczycki, C.J., Geer, R.C., Madej, T., Phan, L.,
977 Ward, M., Lu, S., Marchler, G.H. *et al.* (2020) iCn3D, a web-based 3D viewer for sharing
978 1D/2D/3D representations of biomolecular structures. *Bioinformatics*, **36**, 131-135.
979 25. Pettersen, E.F., Goddard, T.D., Huang, C.C., Meng, E.C., Couch, G.S., Croll, T.I., Morris,
980 J.H. and Ferrin, T.E. (2021) UCSF ChimeraX: Structure visualization for researchers,
981 educators, and developers. *Protein Sci*, **30**, 70-82.
982 26. Mistry, J., Chuguransky, S., Williams, L., Qureshi, M., Salazar, G.A., Sonnhammer, E.L.L.,
983 Tosatto, S.C.E., Paladin, L., Raj, S., Richardson, L.J. *et al.* (2021) Pfam: The protein
984 families database in 2021. *Nucleic Acids Res*, **49**, D412-D419.
985 27. Price, M.N. and Arkin, A.P. (2017) PaperBLAST: Text Mining Papers for Information
986 about Homologs. *mSystems*, **2**.
987 28. Madej, T., Lanczycki, C.J., Zhang, D., Thiessen, P.A., Geer, R.C., Marchler-Bauer, A. and
988 Bryant, S.H. (2014) MMDB and VAST+: tracking structural similarities between
989 macromolecular complexes. *Nucleic Acids Res*, **42**, D297-303.
990 29. Wahba, H.M., Lecoq, L., Stevenson, M., Mansour, A., Cappadocia, L., Lafrance-Vanasse,
991 J., Wilkinson, K.J., Sygusch, J., Wilcox, D.E. and Omichinski, J.G. (2016) Structural and
992 Biochemical Characterization of a Copper-Binding Mutant of the Organomercurial Lyase

993 MerB: Insight into the Key Role of the Active Site Aspartic Acid in Hg-Carbon Bond
994 Cleavage and Metal Binding Specificity. *Biochemistry*, **55**, 1070-1081.
995 30. Johnson, E., Nguyen, P.T., Yeates, T.O. and Rees, D.C. (2012) Inward facing
996 conformations of the MetNI methionine ABC transporter: Implications for the
997 mechanism of transinhibition. *Protein Sci*, **21**, 84-96.
998 31. Abhyankar, W.R., Zheng, L., Brul, S., de Koster, C.G. and de Koning, L.J. (2019) Vegetative
999 Cell and Spore Proteomes of Clostridioides difficile Show Finite Differences and Reveal
1000 Potential Protein Markers. *J Proteome Res*, **18**, 3967-3976.
1001 32. Charlton, T.M., Kovacs-Simon, A., Michell, S.L., Fairweather, N.F. and Tate, E.W. (2015)
1002 Quantitative Lipoproteomics in Clostridium difficile Reveals a Role for Lipoproteins in
1003 Sporulation. *Chem Biol*, **22**, 1562-1573.
1004 33. Saier, M.H., Reddy, V.S., Moreno-Hagelsieb, G., Hendargo, K.J., Zhang, Y., Iddamsetty, V.,
1005 Lam, K.J.K., Tian, N., Russum, S., Wang, J. *et al.* (2021) The Transporter Classification
1006 Database (TCDB): 2021 update. *Nucleic Acids Res*, **49**, D461-D467.
1007 34. Haft, D.H., DiCuccio, M., Badretdin, A., Brover, V., Chetvernin, V., O'Neill, K., Li, W.,
1008 Chitsaz, F., Derbyshire, M.K., Gonzales, N.R. *et al.* (2018) RefSeq: an update on
1009 prokaryotic genome annotation and curation. *Nucleic Acids Res*, **46**, D851-D860.
1010 35. Kim, H.Y., Zhang, Y., Lee, B.C., Kim, J.R. and Gladyshev, V.N. (2009) The selenoproteome
1011 of Clostridium sp. OhILAs: characterization of anaerobic bacterial selenoprotein
1012 methionine sulfoxide reductase A. *Proteins*, **74**, 1008-1017.
1013 36. Hwang, S., Choe, D., Yoo, M., Cho, S., Kim, S.C., Cho, S. and Cho, B.K. (2018) Peptide
1014 Transporter CstA Imports Pyruvate in Escherichia coli K-12. *J Bacteriol*, **200**.
1015 37. Cravedi, P., Mori, G., Fischer, F. and Percudani, R. (2015) Evolution of the
1016 Selenoproteome in Helicobacter pylori and Epsilonproteobacteria. *Genome Biol Evol*, **7**,
1017 2692-2704.
1018 38. Lee, D.Y., Ahn, B.Y. and Kim, K.S. (2000) A thioredoxin from the hyperthermophilic
1019 archaeon Methanococcus jannaschii has a glutaredoxin-like fold but thioredoxin-like
1020 activities. *Biochemistry*, **39**, 6652-6659.
1021 39. Cave, J.W., Cho, H.S., Batchelder, A.M., Yokota, H., Kim, R. and Wemmer, D.E. (2001)
1022 Solution nuclear magnetic resonance structure of a protein disulfide oxidoreductase
1023 from Methanococcus jannaschii. *Protein Sci*, **10**, 384-396.
1024 40. Jeoung, J.H. and Dobbek, H. (2018) ATP-dependent substrate reduction at an [Fe8S9]
1025 double-cubane cluster. *Proc Natl Acad Sci U S A*, **115**, 2994-2999.
1026 41. Jeoung, J.H., Martins, B.M. and Dobbek, H. (2020) Double-Cubane [8Fe9S] Clusters: A
1027 Novel Nitrogenase-Related Cofactor in Biology. *Chembiochem*, **21**, 1710-1716.
1028 42. Hans, M., Buckel, W. and Bill, E. (2008) Spectroscopic evidence for an all-ferrous [4Fe-
1029 4S]0 cluster in the superreduced activator of 2-hydroxyglutaryl-CoA dehydratase from
1030 Acidaminococcus fermentans. *J Biol Inorg Chem*, **13**, 563-574.
1031 43. Parks, J.M., Johs, A., Podar, M., Bridou, R., Hurt, R.A., Jr., Smith, S.D., Tomanicek, S.J.,
1032 Qian, Y., Brown, S.D., Brandt, C.C. *et al.* (2013) The genetic basis for bacterial mercury
1033 methylation. *Science*, **339**, 1332-1335.
1034 44. Smith, S.D., Bridou, R., Johs, A., Parks, J.M., Elias, D.A., Hurt, R.A., Jr., Brown, S.D., Podar,
1035 M. and Wall, J.D. (2015) Site-directed mutagenesis of HgcA and HgcB reveals amino acid
1036 residues important for mercury methylation. *Appl Environ Microbiol*, **81**, 3205-3217.

1037 45. Liu, Y., Chen, H., Van Treuren, W., Hou, B.H., Higginbottom, S.K. and Dodd, D. (2022)
1038 Clostridium sporogenes uses reductive Stickland metabolism in the gut to generate ATP
1039 and produce circulating metabolites. *Nat Microbiol*, **7**, 695-706.
1040 46. Sebaihia, M., Wren, B.W., Mullany, P., Fairweather, N.F., Minton, N., Stabler, R.,
1041 Thomson, N.R., Roberts, A.P., Cerdeno-Tarraga, A.M., Wang, H. *et al.* (2006) The
1042 multidrug-resistant human pathogen Clostridium difficile has a highly mobile, mosaic
1043 genome. *Nat Genet*, **38**, 779-786.
1044 47. Haft, D.H. (2015) Using comparative genomics to drive new discoveries in microbiology.
1045 *Curr Opin Microbiol*, **23**, 189-196.
1046 48. Berry, M.J. and Ralston, N.V. (2008) Mercury toxicity and the mitigating role of
1047 selenium. *Ecohealth*, **5**, 456-459.
1048

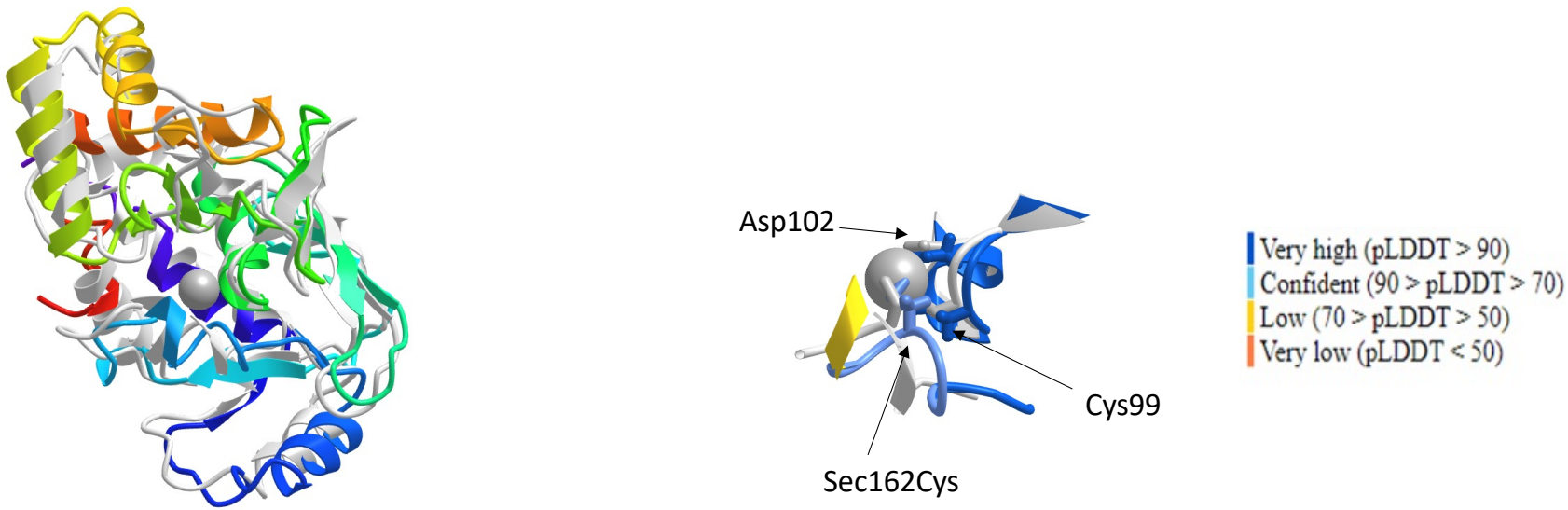

Figure 1: AlphaFold2 structure of $SaoM_{Cdiff}$Sec162Cys with structural alignment to MerB structure 3F0P. The left panel shows alignment of the complete structures, with SaoM colored red-to-purple from N-terminus to C-terminus, while MerB is colored gray. The right panel shows a closeup surrounding the Hg atom bound by MerB. Both MerB and the Hg atom are gray, while $SaoM_{Cdiff}$Sec162Cys is colored by AlphaFold2 pLDDT scores of local structural prediction confidence (see key). Cys99, Asp102, and Sec162Cys (indicated by arrows) align to MerB active site residues Cys96, Asp99, and Cys159.

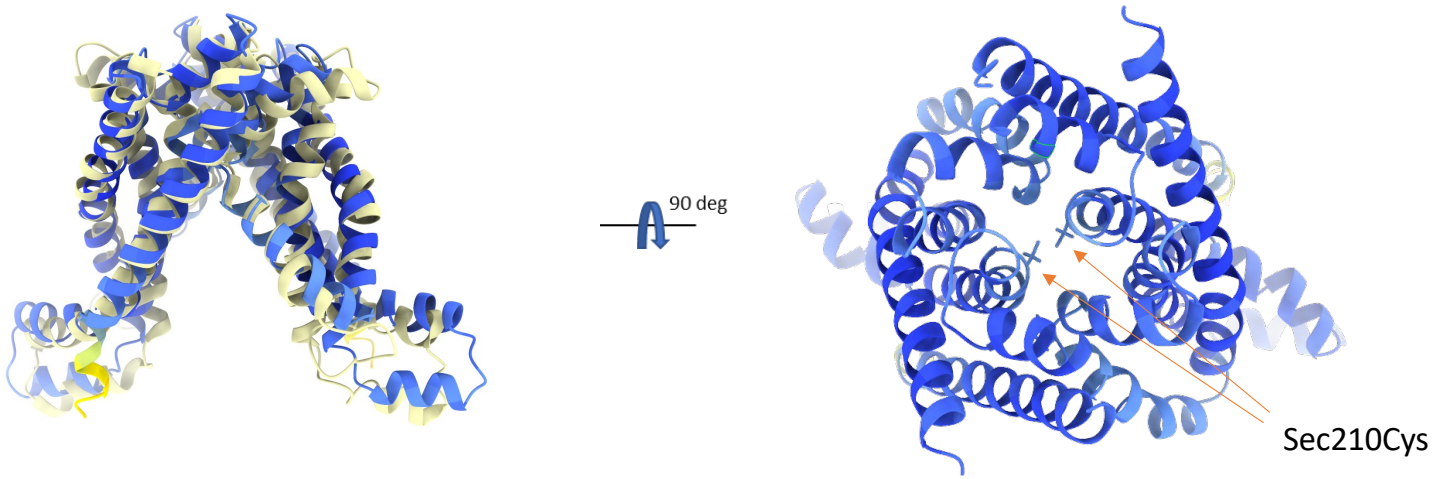

Figure 2: AlphaFold2 prediction for $SaoP_{Cdiff}$Sec210Cys as a homodimer and structural alignment to structure 3DHW for the Escherichia coli ABC transporter permease subunit MetI in the open-inwards conformation. The left panel shows a side view, with the bottom facing the cytosol. The right panel shows a view of homodimeric $SaoP_{Cdiff}$Sec210Cys as seen top-down from outside the plasma membrane after rotation 90^0. Amino acid side chains are shown only for the Cys residue that represents Sec210, which occupies that same position in the center of the image as the permease-gating residue Met-163 in the MetI solved structure.

AlphaFold2 predictions for SaoB and SaoX

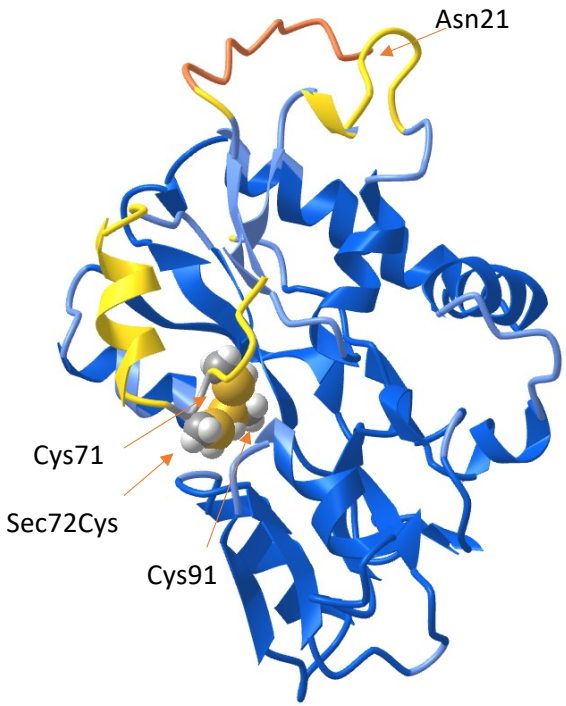

SaoB WP_239591066.1(Sec72Cys)

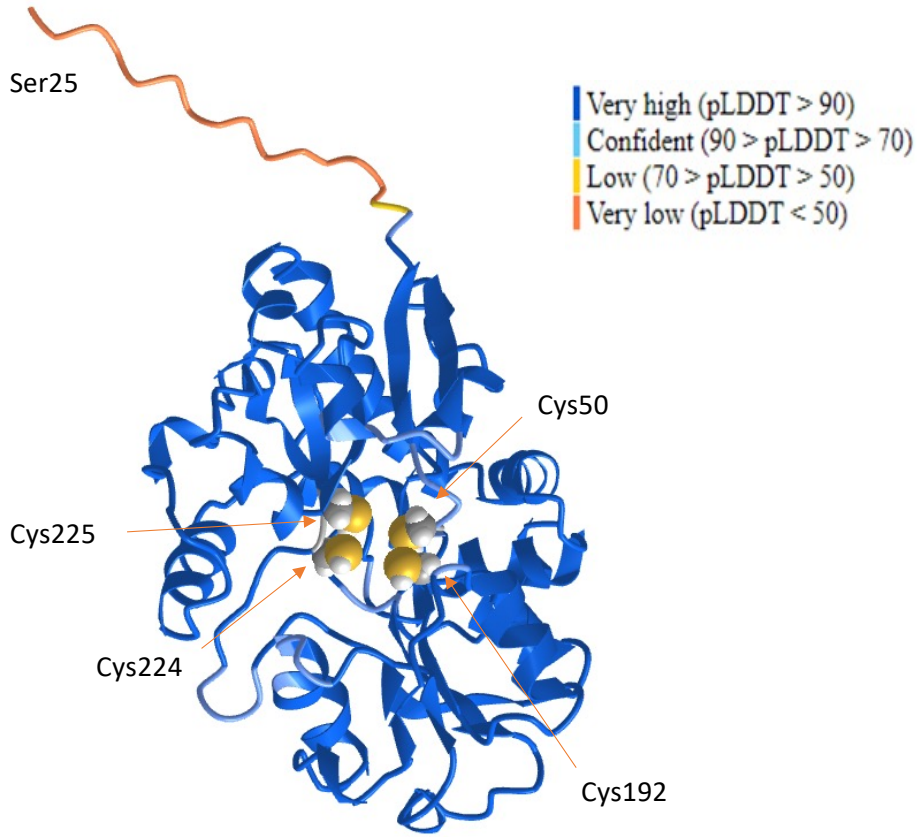

SaoX WP_004454662.1

Figure 3

Figure 3 (legend). AlphaFold2 predicted structures for putative ABC transporter organometallic substrate-binding proteins SaoB and SaoX. Coloring reflects the pLDDT metric of confidence in the local structure. The left panel shows a prediction based on *C. difficile*'s SaoB selenoprotein WP_239591066.1, after trimming an N-terminal signal sequence and replacing Sec72 with Cys. Locations are shown for Cys/Sec residues conserved across the SaoB family, found at positions 71, 72, and 91. All S/Se atoms are near each other and may help form a metal-binding site in a substrate-binding pocket or cleft. A fourth Cys residue is not shown because it is not well conserved in a multiple alignment of SaoB sequences. The right panel shows the lipoprotein SaoX of *C. difficile*, WP_004454662.1, after trimming the predicted lipoprotein signal peptide. An additional N-terminal region is predicted with low confidence (reddish-orange color) and not made part of the globular structure. The rest packs in a structure highly similar to ABC transporter substrate-binding protein PDB structures, such as 4NMY and 2X26. Four conserved Cys residues are found at positions 50, 192, 224, and 225, and their side chains conserve to form what again appears to be a metal-binding site. In about 40% of SaoX proteins, the residue preceding Cys-192 is cysteine as well, forming a CC motif.

Clostridium botulinum strain NCTC 13319: RefSeq annotation of NZ_CP046450.1 from 2931388 to 2941900, with Selenocysteine-Assisted Organometallic (SAO) and double-cubane regions

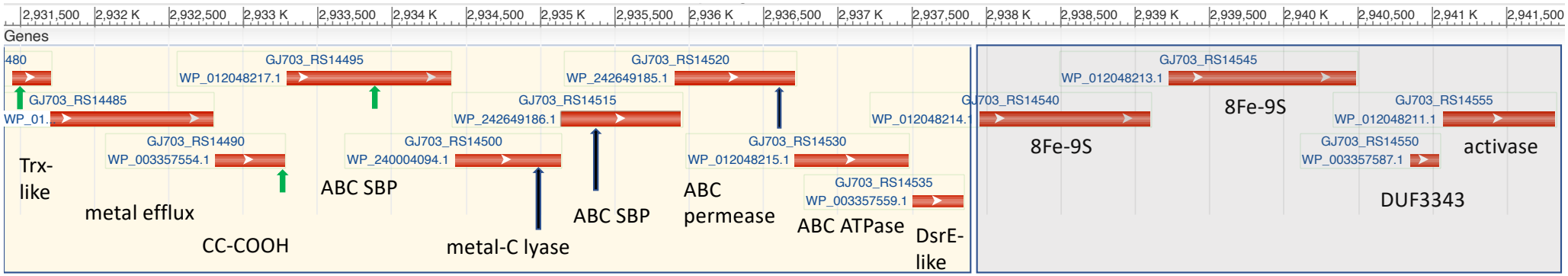

Figure 4: PGAP annotation of the 9-gene *sao* (Selenocysteine-Assisted Organometallic) operon and adjoining double-cubane protein locus in *Clostridium botulinum* strain NCTC 13319. The region shown is from RefSeq nucleotide sequence NZ_CP046450.1 (2931388-2941900). The SAO (selenocysteine-assisted organometallic) locus (yellow box) gene order is *saoTECXLBPAD*. Black vertical arrows show selenocysteine (Sec) insertion codons in *C. botulinum*. Short green vertical arrows show locations where Sec occurs in orthologs from other species. C. botulinum was selected from among 21 *sao* locus-containing representatives with nearby double cubane proteins and their activase (gray box). A comparable re-annotated *sao* region in *C. difficile,* NZ_JAGIVI010000014.1(60051-66700), has four selenoproteins instead of three, with the genes in a different order, *saoDTECXBPAL* (not shown). The lone 8Fe-9S double-cubane protein in that genome, WP_004454390, is located more than 500,000 base pairs away.

CU (Cys-Sec) motif in SaoL (MerB-like)

```
WP_087258257.1 | 149 | 180 | ILHADLKASDNWASCCCCQMLYFNSQADYDAY
WP_238476746.1 | 146 | 177 | VLHINLDKHLNWAASCUNIMNFFWTKSDFDAW
WP_242825830.1 | 146 | 177 | VLHINLDKHSEWAASCUNIMNFFWTKDEYESW
WP_238476748.1 | 146 | 177 | IIHVDLLKNTDWANACUNIMNFFWTKNDLEAW
WP_238476750.1 | 146 | 177 | VIHVDLNKNKNWASTCUNIMNFFGSKNDMNEW
WP_238493462.1 | 161 | 192 | ILHVDLNKNKNWSGECUNIMNFFCRKNEYDEW
WP_238493470.1 | 157 | 188 | VLHVDLNKNQNWSGSCUNIMNFFCKKEHYDQW
WP_246565854.1 | 159 | 190 | ILHVDLNKNSNWSGSCUNVMNFFCKEKEYNVW
WP_238493466.1 | 158 | 189 | VLHVDLNQIDDWAASCUNIMNFFCTKNHYNEW
WP_240004101.1 | 173 | 204 | VLHVDLNKNDSWASSCUNIMYFFCSEEHYRNW
WP_238493465.1 | 151 | 182 | ALHVDLNKHTDWGTTCUNIMNFFCTEKDFDIW
```

CU motif in substrate-binding protein SaoB

```
WP_004608618.1 | 66 |  97 | HQSSSFQDCCSNTAQWAMNAKEINVGFYCTHI
WP_169300993.1 | 78 | 109 | LEFYTFKDCCSNTAQWALTAKEIDMAFYCNHM
WP_239591073.1 | 68 |  99 | MEGYEFQDCUSNTAQWALRSEEIDMALSCSHQ
WP_087258574.1 | 74 | 105 | LDSYLFIDCCSNAGQWSLLTQDIDLGFYCSHI
WP_011700728.1 | 65 |  96 | YDPYVMKDCCAGTSEWAFGTNRLDVALMCPDA
WP_146164898.1 | 69 | 100 | YEIFSLEDCCAAISQFALLSLAVDAAILCPTA
WP_039879528.1 | 70 | 101 | LSFLQLSDCCGTQAEFALAGGDFDMAVLCPDA
WP_031483264.1 | 62 |  93 | IKTFQINDCCTPVAQWAMSSQSVDLALMCPDS
WP_050355227.1 | 63 |  94 | FETYSIKDCCSNTSQWALTSDLLDISILCPDA
WP_239591069.1 | 64 |  95 | FEPYFIKDCUDNTSQWALSSDVLDIAIMCPEA
WP_251861114.1 | 64 |  95 | FEPYFIKDCUGNTSQWALSSDVLDMAIMCPEA
WP_239591067.1 | 59 |  90 | LEAYFIKDCUAKTSQWALSSDMLDMAIVCKEA
WP_239591062.1 | 65 |  96 | LEPYSINDCUASTMQWALSSDQIDMAIICKEA
WP_239591063.1 | 65 |  96 | IETYSINDCUASTMQWALSSEQIDMAIICKEA
WP_245398079.1 | 66 |  97 | MDTFTINDCUASTMQWALSSEEIDIAIICKDA
WP_239591072.1 | 64 |  95 | IDSYSIADCUSASMQWALSSDEMDMAIICKDA
WP_239591068.1 | 65 |  96 | VESYILGDCUSPSAQWALSSDSVDMAIICPDS
```

CU motif at the C-terminus of SaoC

```
WP_227186491   | 148 | 180 | VTGEKNGAVGYAIYRIIDG-EMVDLFGEGMEDCC
WP_044937124.  | 153 | 185 | ITGEKNGAVGYAIYRMIDG-APTDLFGEGMEDCC
WP_005334080.  | 148 | 180 | ITGEKKGAVGYAIYRMIDG-QPVDLFGEGMEDCC
WP_087258577   | 145 | 177 | VTGEKDGEVGYAIYRIIDG-ELINLFGEDMEDCC
WP_252346670   | 173 | 205 | LQGQKGSNVGYGIFRVVDG-SPVNLFGEGMEDCU
WP_252346669   | 168 | 200 | LQGQKGAKVGYGIFRVIEG-KAVNLFGEGMEECU
WP_252346671   | 168 | 200 | LQGQKGSKVGYGIYRVIDG-ALVNLFAEGLQECU
WP_009214287.  | 134 | 166 | ITGEKNGKLGYAVYRIIDG-SFKDLFGEGMKDCC
WP_093314495   | 124 | 156 | ISGSKGPHVGHAIYRIVDD-ELVDLFSMDMSLCC
WP_093371958   | 122 | 154 | ISGSKGPHVGHAIYRIVDG-ELVDLFSMDMSLCC
WP_252346672   | 129 | 161 | VSGSKRGQYGYGIFR-IEDKHLHNLFSEGMGVCU
WP_028329263.  | 117 | 149 | VSGQKGANIGFAVYRLENG-QLISLFENGMEKCC
WP_157150838   | 116 | 148 | VSGKKGANIGFAVYRLENG-EFISLFENGMEKCC
WP_096737795   | 118 | 150 | VSGKKGAHIGFAVYRLENG-EFISLFENGMEDCC
WP_147736609   | 118 | 150 | VSGQKGANIGFAVYRLENG-EFISLFESGMERCC
WP_008520778.  | 118 | 150 | VSGQKGIHIGFAVFRFVEG-KWISLFGEGMEDCC
WP_015556509.  | 124 | 156 | VSGQKGIYIGYAVFRFVDG-EWISLFGDGMDGCC
WP_051677063.  | 124 | 156 | VQGMKGAKSGFAIYRMENG-ELMDVFGEGMEDCC
WP_163340325   | 125 | 157 | VQGMKGAKTGFAIYRFVDG-RIEDVFGEGMDDCC
```

CU motif in HgcA N-terminal extension

```
WP_252396620.1 | 33 | 64 | APPCUGPPTSAGGGEIT-------DQVPGFLGWVAAGSR
WP_250697419.1 | 33 | 64 | APPCUGPRTSAGGGTID-------ETVPGFEGWLDTPAG
WP_250697418.1 | 31 | 62 | KPPCUGPPTSAGGGAIT-------DKVPGFIEWLETPAG
WP_250697417.1 | 38 | 69 | KPPCUGPRPPAGGGIID-------ETVPGFTGWLETQAG
WP_250697416.1 | 11 | 42 | KPPCUGPENSAGGGEIN-------DQVPGFTSWLTTTVG
WP_108102289.1 | 22 | 53 | RPPCCGPPATVGGGEID-------ETVPGFLGWLSTTTG
WP_250697415.1 | 29 | 60 | KEPCUGPKTPAVSGTIN-------ENVPGFIRWHETPAG
WP_245693461.1 | 35 | 73 | AEPCCGSAAEAVGPRWADRERPGYRIWPFVDEWIETPVG
WP_010243111.1 | 41 | 75 | GSCCCGGSDQAEAEPITQY----DKKDNWITGEIKTPRG
WP_207655107.1 | 42 | 76 | SSCCCGNGSSASCEAITKY----DLKEKWIIGEISTPAG
WP_004626173.1 | 44 | 78 | NTCCCGGSDNCSSEPVTNY----DRNIPWITGEIETAAG
WP_200881740.1 | 37 | 72 | DAVCCGEPPGPRSNPDEKPGY---ELQHYVDSFLDSPMG
WP_205232271.1 | 31 | 66 | QEVCCGGAPPPKTNPLERPGY---TLKPFVRAFIKDSRS
WP_236890013.1 | 18 | 53 | EPCCCGPAPSPRSDGRELPGY---KLCGFVASFMETPAD
WP_252396623.1 | 24 | 59 | EEICUGPQPDPEAGVYERPGY---DICGFVEEFMETPAG
WP_250697406.1 | 31 | 66 | QAPCUGPNAEPRAGVHEKAGY---SIDAYVEGFIDTPVG
WP_250697404.1 | 23 | 58 | EAPCUGPKPEPRSGVHERAGY---SLCPFVTGFIDTPAG
WP_250697405.1 | 25 | 60 | EAPCUGPKQEPRAGVDQRAGY---CIEPFVEQFMATSIG
WP_250697407.1 | 25 | 60 | SGPCUGPETYPRAGEHEKAGY---TIDPFVHGFIQTARG
WP_252409333.1 | 36 | 71 | EEPGUGPRPGPGFGPENKPGY---TVCHFVRDFARTPVG
WP_252396621.1 | 38 | 73 | NAPCUGPKTESGFGVYDKPGY---TISPFIESFYETPGG
```

Figure 5. Cys-Sec motifs in key proteins of SAO and methylmercury metabolism

Figure 5: Alignments of selenoprotein and non-selenoprotein versions of proteins SaoL (top left), SaoB (top right), SaoC (bottom left), and HgcA (bottom right), for short regions that include the site where the selenocysteine may occur, are show as displayed in belvu (18), colored by residue type. For SaoL, homolog of the organomercurial lysase MerB, the top sequence (WP_087258257.1) was exceptional for having Cys (C) rather than Sec (U), and the site is "packed", with four consecutive Cys residues. Similar packing with extra Cys residues is seen in methyl mercury formation protein HgcA region. Full-length multiple sequence alignments for all eight selenoprotein families described in this paper can be found in Supplemental Materials.